Physical Processes in Geological Carbon Storage

An Introduction with Four Basic Posters

by

K.U.Weyer, Ph.D., P.Geol., P.HG.

WDA Consultants Inc., Calgary
weyer@wda-consultants.com

WKC Consultants, Krefeld
weyer@wkc-consultants.com

March 3, 2010
corrected March 2, 2015

Table of Contents

Summary portion of
E.O.Frind and J.W.Molson, 2010. Review of "Physical Processes in Carbon Storage" by Udo Weyer. January 11, 2010. 16 Pages (Summary 1 p.)

Chapter 1

Introduction

An invitation by the Brazilian petroleum company PetroBras to their September 2008 CO_2 Seminar in Salvador, Brazil, caused me to integrate Hubbert's Force Potential (Hubbert, 1940) and the Theory of Gravitational Groundwater Flow Systems (Tóth, 1962) to the geological storage of CO_2. Both theories are physically consistent and have been tested in many practical cases throughout the world by the oil industry and hydrogeologists for more than 40 years. Both geophysicists by training, Hubbert worked in the exploration end of Shell, while Tóth was at the time employed by the Alberta Research Council.

Building on the misdirecting influence of Muskat (1937), reservoir engineering applies the methods of continuum mechanics (energy related to volume) to fluid flow within oil fields. At the time, Hubbert realized that Muskat's (1937) approach was physically inconsistent and lacked physical causality (Hubbert, 1969; see Introduction) and, in response, put together the 1940 treatise presenting physically-consistent derivations for subsurface fluid flow. Hubbert's Force Potential relates energy to mass. Hubbert (1953) subsequently applied force potential treatment of all subsurface fluid flow to the exploration for petroleum. The basic equations of Hubbert's Force Potential are shown in the introduction to chapter 5 (Poster 4).

The subsequent development of the Theory of Groundwater Flow Systems was based on Hubbert's force potential and on practical oilfield data, namely on the strange behaviour of water level data (head levels) in boreholes drilled by cable tools without mud circulation in the Turner Valley oil field southwest of Calgary [poster 1; chapter 3]. These water level data were then evaluated with respect to the topography of the groundwater table and to the depth and permeability of geologic layers encountered. It turned out that, due to thermodynamic reasons of minimizing the total energy consumption, regional groundwater flow systems penetrate aquitards (caprocks in oil field terminology) on their way from recharge areas to discharge areas and may reach great depths in doing so. These conclusions were also based on the results of 2D vertical mathematical models applying Hubbert's force potential [poster 2; chapter 3].

Hubbert (1953) showed that the force field of fresh groundwater determines the natural flow directions of liquid and gaseous hydrocarbons at depth. Fresh groundwater force fields exert the same effect on injected CO_2. Weyer (1978) deduced under which hydrodynamic and geological conditions the so-called 'buoyancy forces' will be directed downwards. Under these conditions fluids lighter than water (including gaseous fluids) will move downwards faster than both water and fluids denser than water [poster 3; chapter 4]. Weyer (1978) named the effect of these conditions *Buoyancy Reversal* [short: BR]

Under hydrostatic conditions the value of the mechanical hydraulic gradient (-grad Φ) is zero. Therefore no gravity-driven flow takes place. Such conditions exist at StatoilHydro's off-shore CO_2 injection site Sleipner. At Encana's on-shore CO_2 injection site, Weyburn, and other on-shore sites -grad Φ is unequal to zero and gravity-driven flow and hydrodynamic conditions

exist. Hence naturally occurring *Buoyancy Reversal* only occurs on-shore. In both environments, on-shore and off-shore, *Buoyancy Reversal* can perceivably be created by hydrocarbon production and other persistent pumping from deep wells.

Poster 4 [chapter 5] deals with the trapping of CO_2 by means of subsurface water flow through the mechanism of *Buoyancy Reversal*. This new trapping mechanism establishes the whole thickness of an aquitard (caprock) as a barrier to upward movement of CO_2 and not just the thin boundary layer exerting capillary forces. Moreover any breakthrough of CO_2 near the injection site due to increased pressure potentials under the caprock can be prevented by increasing the pressure potential above the top of the aquitard (caprock). In doing so one could use hydrous fluids from the lower part of the injection layer and thus increase, as a beneficial effect, the injection layer's storage capacity for injected CO_2. As the pressure potential will dissipate from the injection site towards the surroundings, the pressure at the injection site will be reduced upon cessation of injection and thereby allow eventual discontinuation of water injection above the caprock.

The posters collected here explain, in condensed form and with straightforward terminology, the physical concepts of Hubbert's Force Potential, of gravitational groundwater flow systems, of *Buoyancy Reversal* and its application to an improved geological storage of CO_2.

Posters 1 and 2 [chapter 3 and 4] were written as introduction into the Theory of Gravitational Groundwater Flow Systems, which forms one of the pillars for the subsequent posters 3 and 4. Poster 3 was first presented and discussed at SEG 2009 Summer Research Workshop: CO_2 Sequestration Geophysics, Banff, Alberta, Canada, 23-27 August, 2009. Posters 4 was first presented and discussed at the ESF Conference 'CO_2 Geological Storage – Latest Progress' in Obergurgl, Austria, 22-27 November 2009 together with Poster 3. In addition, Posters 3 and 4 have also been presentated and discussed at the GCEP/USGS participatory workshop 'Caprocks and Seals for Geologic Carbon Sequestration' in Monterey, CA, USA, January 12-15th, 2010.

Chapter 6 determines the magnitude of the hydraulic gradient (-grad Φ), which, under conditions of vertically downward directed flow, forms the threshold between conditions with pressure potential increasing with depth and the conditions of pressure potential decreasing with depth (*Buoyancy Reversal*). It also presents a basic diagram relating the occurrence of *Buoyancy Reversal* to the amount of downward flux and permeability. Both the above threshold value and the basic diagram were first shown during discussions at the Obergurgl conference. The numbers and diagrams have been derived and calculated in a physically consistent manner by applying Hubbert's Force Potential and summarizing tables of Weyer (1978, 1996). Field data from Hitchon et al. (1989a, 1989b) and Bachu et al. (1993) establish the natural occurrence of *Buoyancy Reversal* in regionally extended downward flow sections under large regional groundwater recharge areas in Alberta. The extent of areas with downward flow at depth (under uplands) is often much larger than areas with upward flow (under valleys and lowlands). This is shown by Fig. 8 and 10 (Ch. 4) and 4 and 6 (Ch. 5). All of the Swan Hills are an extended upland area with strong downward flow penetrating the Clearwater-Willrich Aquitard (the layer with naturally occurring *Buoyancy Reversal*) while, under pre-petroleum production

conditions, the deep-seated upward flow through the same aquitard occurred only in a limited area under the valley of the Athabasca River.

Chapter 7 elaborates on the presence of hydrostatic conditions at off-shore sites like Sleipner in the North Sea and the presence of hydrodynamic conditions at on-shore sites like Weyburn, Saskatchewan, and Zama Lake and Wabamun, both located in Alberta, Canada. Hence the flow behaviour of the CO_2 at the Sleipner site cannot be taken as a precedent for the Weyburn site or other on-shore sites. The chapter also presents a road map for future investigations applying physically-consistent methods to CO_2 storage.

Chapter 8 provides a roadmap for integrating and applying Hubbert's force potential and *Buoyancy Reversal* to the geological storage of CO_2.

Appendix 1 presents the summary of a 16 page review of the above chapters 1 to 7 (version December 21, 2009) by two eminent hydrogeological modellers, Emil Frind of the University of Waterloo, Ontario, and John Molson of Laval University, Quebec (Frind & Molson, 2010). The full review with the detailed coments is available from the website www.wda-consultants.com. In response to the review I have corrected the use of the term "principle" (Dec.21, 2009 version: p.11, last line) to read "principal flow patterns" and changed "removal" (Dec.21, 2009 version: p. 29, line 3) to "reversal". In Figure 1 (chapter 6) the labelling error discovered in the review has been corrected.

I appreciate Emil's and John's unsolicited review efforts immensely, in particular as their mathematical models confirmed the occurrence of *Buoyancy Reversals* which I had first derived from theoretical considerations (Weyer, 1978) and later confirmed by field data (taken from Hitchon et al., 1989a, Hitchon et al., 1989b, and Bachu et al., 1993).

With respect to my use of the term *Buoyancy Reversal* and the proposal by Frind and Molson (2010) to use the term "pressure gradient reversal" instead, I find my term to be more suited to express the physical meaning that the so-called "buoyancy forces" are directly dependant on the pressure potential forces and therefore, in a hydrodynamic environment, follow the non-vertical directions of the pressure potential force vector. The opinion that so-called vertically upwards directed buoyancy forces would be an omnipresent force for lighter parcels within fluids is erroneous.

The term *Buoyancy Reversal* relates closely to the physics of force fields involved. The so-called "buoyancy forces" are created by pressure potential forces (see chapters 5 and 6) which in the hydrostatic case happen to be directed upwards. Under general hydrodynamic conditions the same pressure potential forces may be directed in any direction in the subsurface including downwards. Downwards directed pressure potential forces may then lead to *Buoyancy Reversal*.

The concept applied assumed strong vertically downwards-directed flow through a three layer system with an low permeable aquitard sandwiched between two aquifers (chapter 4: Figure 7).

In both aquifers the pressure potential force (the buoyancy force) is directed upwards, while the pressure potential force within the aquitard is directed downwards. Ergo what is commonly considered to be the "buoyancy force" has been reversed. Under these conditions lighter parcels would move downwards faster than heavier parcels, in contrast to common experience in hydrostatic conditions. One always should keep in mind that Hubbert's force potential mainly consists of two physical fields: the gravitational energy field and the pressure potential energy field (which in the subsurface is derived from the gravitational field).

Frind and Molson (2010) followed my opinion and make the point that all simulations need to be based on head values and gradients not on pressure gradients. They (ibid) agree that simulators which take caprocks as top model boundaries are unsuitable for modelling CO_2 sequestration.

References

Bachu, S., J.R. Underschultz, B. Hitchon, and D. Cotterill, 1993. Regional-Scale Subsurface Hydrogeology in Northeast Alberta. Alberta Research Council, Bulletin No. 61.

Frind, E.O. and J.W.Molson, 2010. Review of 'Physical Processes in Carbon Storage" by Udo Weyer. January 11, 2010. 16 p. *[available from http://www.wda-consultants.com]*

Hitchon, B., C.M. Sauveplane, S. Bachu, E.H. Koster, and A.T. Lytviak, 1989a. Hydrogeology of the Swan Hills Area, Alberta: Evaluation for deep waste injection. Alberta Research Council Bulletin No. 58 [*Dec 2009: available electronically at no charge from AGS-info@ERCB.ca*].

Hitchon, B., S. Bachu, C.M. Sauveplane, A. Ing, A.T. Lytviak, and J.R. Underschultz, 1989b. Hydrogeological and geothermal regimes in the Phanerozoic succession, Cold Lake area, Alberta and Saskatchewan. Alberta Research Council Bulletin No. 59 [*Dec 2009: available electronically at no charge from AGS-info@ERCB.ca*].

Hubbert, M. King, 1940. The theory of groundwater motion. J.Geol., vol.48, No.8, p.785-944.

Hubbert, M. King, 1953. Entrapment of petroleum under hydrodynamic conditions. The Bulletin of the American Association of Petroleum Geologists, vol. 37, no. 8, p. 1954-2026.

Muskat, M., 1937. The flow of homogeneous fluids through porous media. McGraw-Hill.

Tóth, J., 1962. A theory of groundwater motion in small drainage basins in Central Alberta, Canada. J. Geophys. Res., vol.67, no.1, p.4375-4387.

Weyer, K.U., 1978. Hydraulic forces in permeable media. Mémoires du B.R.G.M., vol. 91, p.285 - 297, Orléans, France *[available from http://www.wda-consultants.com]*

Weyer, K.U., 2009. Applying Hydrogeological Methods and Hubbert's Force Potential to Carbon Storage: A Primer. 23 pages of introductory text followed by 68 pages containing 135 slides. [available from http://www.wda-consultants.com.]

Chapter 2

[Poster 1]

Role of Gravitational Groundwater Flow Systems in Carbon Sequestration

K. Udo Weyer
WDA Consultants Inc., Calgary, AB, Canada
weyer@wda-consultants.com

Introduction

The Theory of Groundwater Flow Systems (Tóth, 1962) originated in Alberta, Canada in response to early cable tool drilling data from oil wells in the Turner Valley (Fig. 1), 50 km southwest of Calgary, Alberta.

Fig. 1 Topography at Turner Valley, Alberta, Canada. Water level data from the Turner Valley Oilfield gave rise to the Theory of Groundwater Flow Systems (picture: K.U. Weyer, 20070621)

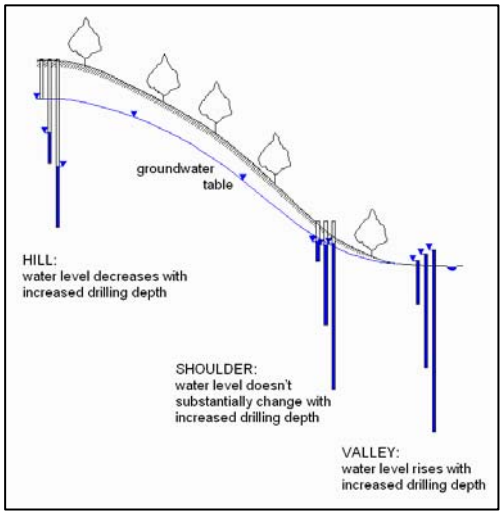

Fig. 2 Behavious of water levels in piezometer nests on hills, slope shoulders, and in valleys.

In the 1920s drilling was done with cable tool rigs without fluid circulation, while almost all other drilling methods used since apply mud or air circulation. The cable tool rig allowed a constant observation of the behaviour of the water level in the borehole with increasing drilling depth. Drilling on hills encountered water levels that decreased with depth once the groundwater table had been reached (Fig. 2). In valleys the water levels rose with drilling depth and turned artesian (flowing). At the shoulder of valleys the water level did not change substantially. This behaviour was puzzling but was finally explained in the 1960s by applying Hubbert's (1940) Force Potential, which up to this time had been widely considered as an absurd opinion within hydrogeology. Thus Hubbert's theoretical development and analytical model of flow within a vertical cross-section (Fig. 3) was confirmed by actual field measurements in the Turner Valley oilfield.

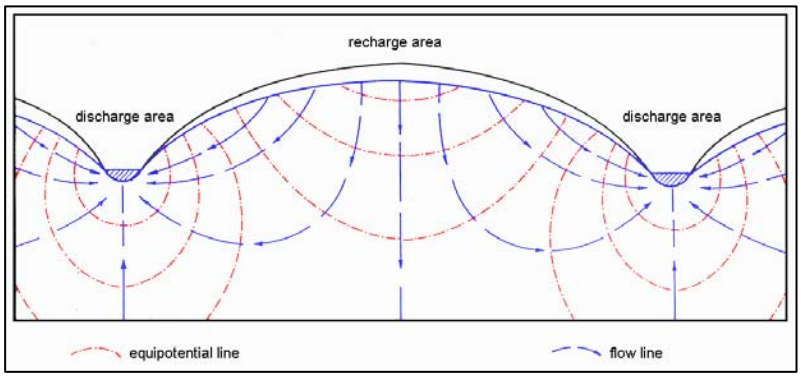

Fig. 3

Energy fields (equipotential lines, small dashes) and flow field (flow lines, long dashes) of groundwater flow through homogeneous and isotropic rock in a cross-section between two valleys (after Hubbert, 1940, Fig. 45)

In Fig. 3, recharge areas occur in the elevated portion of the cross-section and discharge areas in the lowlands (valleys). The vertical flow lines under the top of the recharge area and in the middle of the discharge areas indicate hydraulic boundaries between flow systems. In undisturbed conditions, water does not penetrate from one flow system to another.

Inception of Groundwater Flow Systems Theory

In an attempt to explain additional hydrogeological field evidence, electrical Teledeltos paper models of geological cross-sections and simplified analytical calculations led to the formulation of the principles of Groundwater Flow Systems (Tóth, 1962).

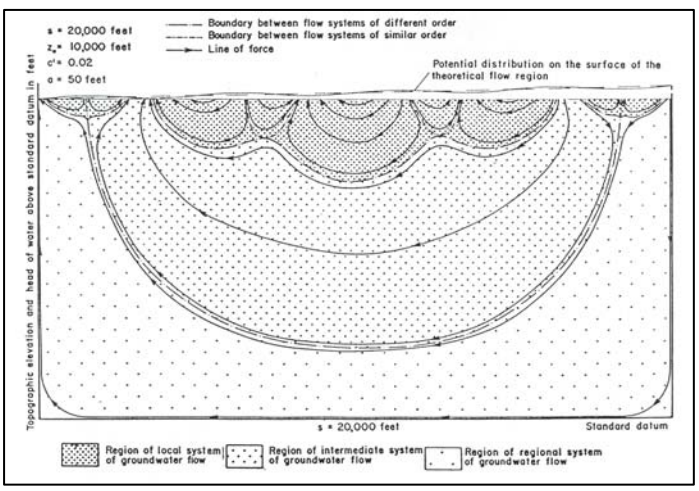

Fig. 4

Mathematical model by Tóth [1962]: analytical calculation of groundwater flow systems in a cross-section with homogeneous and isotropic lithology

Within Tóth's model (Fig. 4), the total elevation gain from the valley to the uppermost hill was taken as approximately 150 m over about 6.5 km; the amplitude between hills and valleys was assumed to be approximately 15 m. The calculations were done analytically in a rectangular field with the undulating boundary condition assigned as the upper boundary to the rectangular field of analytical calculations.

Based on the pattern and discharge points of the flow lines obtained (Fig. 4), Tóth (1962) classified the flow lines of the flow systems into three parts. Local flow systems migrate between neighbouring hills and valleys. In this case, the one intermediate system flows from the second-last hill and discharges into the second-last valley. The regional flow system originates from the highest hill and discharges into the deepest valley.

An important observation is that within flow systems, the direction of groundwater flow could be opposite to the direction of the slope of the groundwater table. This eliminated the use of simple Darcy equations to determine flow directions at greater depth, or the use of the hydrologic triangles to determine the flow direction of groundwater and also the concept of the determination of flow directions by use of pressure values based on the weight of the water column above the point of consideration (as is sometimes assumed in reservoir engineering).

What happened in the development of the Theory of Groundwater Flow Systems is an instructive example of the mutual interplay and reinforcement of theoretical development (Hubbert, 1940), field water level data from oil boreholes in the Turner Valley, and subsequently, additional applications of mathematical models. It becomes obvious that not only can the mathematical model verify and give meaning to the field data, but available field data also can confirm the validity of mathematical models.

In an effort to further understand groundwater flow pattern, Freeze and Witherspoon (1966, 1967) determined the effect of topography and geologic structures of differing permeabilities upon groundwater flow pattern by simulating groundwater flow systems in 2D-vertical geologic cross-sections using early numerical computer models.

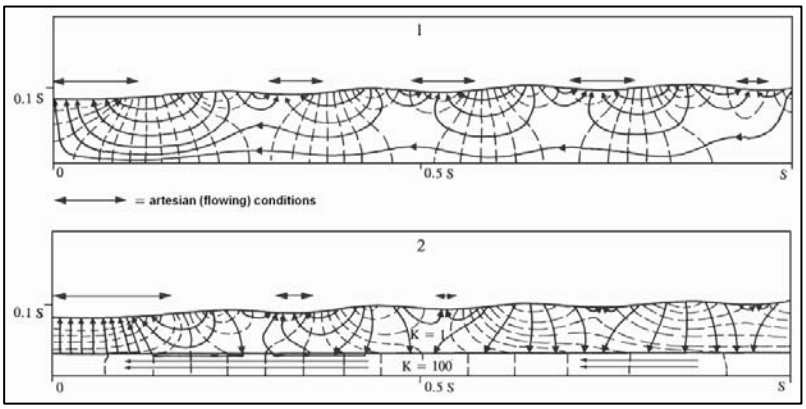

Fig. 5

Mathematical models by Freeze and Witherspoon [1967]: effect of [1] topography and [2] a buried higher-permeable layer upon groundwater flow pattern and location of recharge and discharge areas.

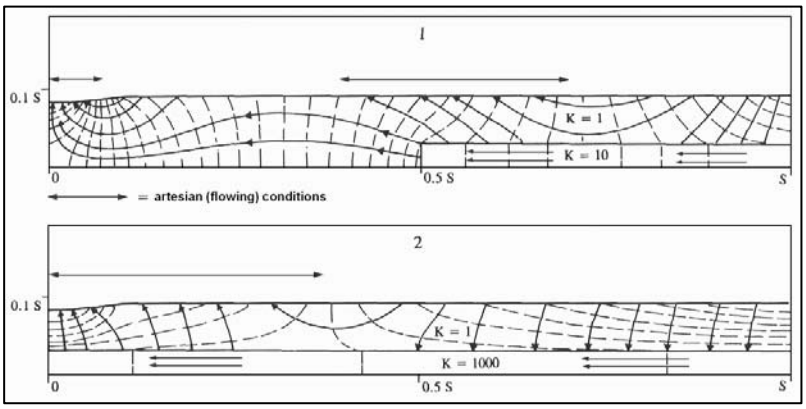

Fig. 6

Mathematical models by Freeze and Witherspoon [1967]: Effect of a buried higher-permeable layer [1,2] upon groundwater flow pattern and location of recharge and discharge areas.

To achieve generally valid results, contrast permeabilities (using relative values), dimensionless distance and dimensionless depth [S] were applied in the model calculations. When using contrast permeabilities, the flow lines are defined properly, but no information is retrieved as to the velocity or amount of groundwater flow. The dimensionless length and depth show that similar flow patterns exist for models of 1, 10 or 50 km length. Also, the location of the aquifer under the aquitard (which is a natural situation in many areas) concentrates the flow into the aquifer, delivering it from the highland area to the lowland area (valley).

Within these mathematical models, geologic layers are homogeneous and isotropic. Again, flow lines show the occurrence of local, intermediate, and regional flow systems (Figure 5 [1]). Evaluating the flow lines in Figure 5 [2], shows approximately twice as much water flowing within the aquitard (down from recharge areas and up towards the discharge area) as within the aquifer (lateral flow only). Figure 6 [2] shows the same pattern of approximately twice as much water flowing through the aquitard vertically down and up, as flows laterally in the aquifer.

In all four figures, the double-sided lateral arrows indicate areas of artesian (flowing) conditions which means areas of upward flow and discharge.

Penetration Depth of Groundwater Flow Systems

In Fig. 4, Tóth shows local flow systems penetrating up to 900 m depth. The one intermediate system penetrated up to 2400 m depth. The regional flow system originating from the highest hill penetrated to a depth of over 3000 m - the lower limit of the mathematical model. Considering the dimensionless lengths and depths used by Freeze & Witherspoon (1967) in their numerical models, penetration depths there could be between 100 m and 5 km, assuming the lengths to be 1 km or 50 km. Similar penetration depths of 5 to 6 km (Fig. 7) are shown by Tóth (2009).

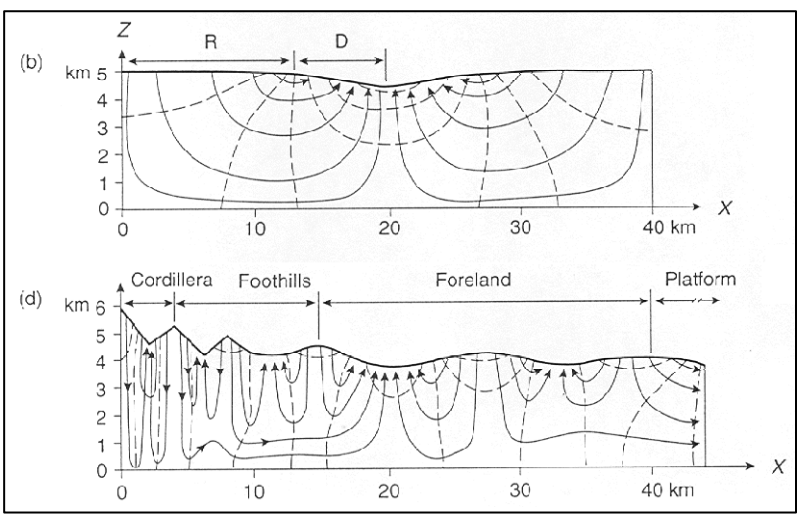

Fig. 7

Schematics of groundwater flow patterns for common types of regional landforms: (b) intracratonic basin with broad uplands; (d) cordillera-cum-foreland.

The schematic topography in case (d) is similar to the situation in Alberta, Canada. All cross-sections are devoid of heterogeneities. The cross-sections have been selected from Tóth (2009), Fig. 3.14.

Hubbert (1953) showed that the force fields of fresh groundwater determine the migration behaviour of oil and gas in the subsurface. This also applies to the storage of CO_2. Hence the knowledge of groundwater flow systems at greater depth, and their force fields, is a cornerstone to understand and determine the migration behaviour of hydrocarbons and CO_2 in the subsurface.

Conclusions

- Water level data in oil boreholes of the Turner Valley oil field gave rise to the Theory of Groundwater Flow Systems when they were interpreted within the realm of Hubbert's Force Potential.
- The penetration depth of groundwater flow systems reaches depths of several kilometers, well within the depth reach of oil fields and carbon storage in reservoirs and saline aquifers.
- The development of the Theory of Groundwater Flow Systems is an instructive example of the mutual interplay and reinforcement of theoretical development, field data, and the subsequent additional applications of mathematical models. Not only can the mathematical model verify and give meaning to the field data, but available field data can also confirm the validity of mathematical models of fluid flow in the subsurface if the models have a base in physics.

References

Freeze, R.A. and P.A. Witherspoon, 1966. Theoretical analysis of regional groundwater flow: 1. Analytical and numerical solutions to the mathematical model. Water Resources Research, vol.2, no.4, p.641-656

Freeze, R.A. and P.A. Witherspoon, 1967. Theoretical analysis of regional groundwater flow: 2. Effect of water table configuration and subsurface permeability variation. Water Resources Research, vol.4, no.3, p.581-590.

Hubbert, M. King, 1940. The theory of groundwater motion. J.Geol., vol.48, No.8, p.785-944.

Hubbert, M. King, 1953. Entrapment of petroleum under hydrodynamic conditions. The Bulletin of the American Association of Petroleum Geologists, vol. 37, no. 8, p. 1954-2026.

Tóth, J., 1962. A theory of groundwater motion in small drainage basins in Central Alberta, Canada. J. Geophys. Res., vol.67, no.1, p.4375-4387.

Tóth, J., 2009. Gravitational systems of groundwater flow: Theory, Evaluation, Utilization. Cambridge University Press, 297 p.

Weyer, K.U., 1978. Hydraulic forces in permeable media. Mémoires du B.R.G.M., vol. 91, p.285-297, Orléans, France *[available from http://www.wda-consultants.com]*.

Chapter 3

[Poster 2]

Modelling of Groundwater Flow Systems within 2D Vertical Cross-Sections

K. Udo Weyer
WDA Consultants Inc., Calgary, AB, Canada
weyer@wda-consultants.com

Introduction

The development of the groundwater flow systems theory was based on 2D models of groundwater flow in geologic cross-sections. These models were not based on actual field data but on theoretical boundary conditions and assumed parameters as contrast permeabilities, layer heterogeneity and isotropic rocks.

The use of contrast permeabilities returned accurate flow lines but not the velocity and amount of groundwater flow. The selection of contrast in permeability proved to very tolerant in the sense that significant differences in contrasts would still return similar flow lines. Also the regional size of the models allowed the groundwater table to be fixed to the topography leading to realistic results in the first model run. The problems associated with assuming recharge rates and numerous repetitions of model runs were thus eliminated.

Numerical Modelling of a 2D Sand Model of a Geologic Cross-Section

Weyer (1996) tested these conditions in laboratory studies and field studies by comparing real world data with the results of singular 2D model runs. Figure 1 shows groundwater flow through a table model with a vertical cross-section of sand layers. Figure 2 shows the result of a first run of a 2D vertical model with contrast permeabilities assumed. The flow lines in Figure 2 [D] reflect the colour plumes within Figure 1 [B, C, D] quite well. This observation confirms that 2D vertical modelling of groundwater flow in geologic cross-sections is effective, tolerant of permeability estimation errors, and returns the principal flow patterns of groundwater flow systems.

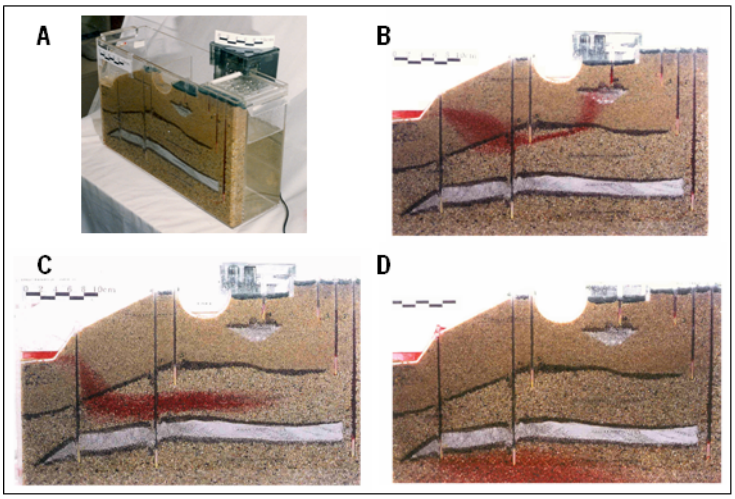

Fig. 1

Sand model of groundwater flow

A: Technical setup
B: Groundwater flow demonstration 1 through geologic cross-section
C: Groundwater flow demonstration 2 through geologic cross-section
D: Groundwater flow demonstration 3 through geologic cross-section

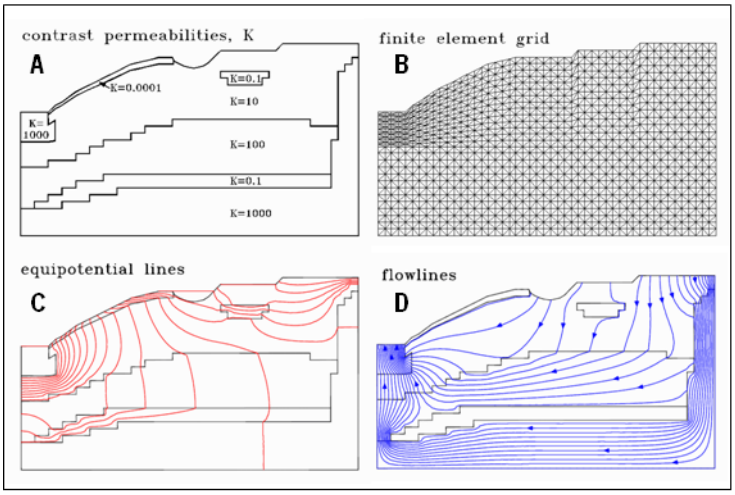

Fig. 2

Mathematical simulation of sand model based

A: on a first estimation of contrast permeabilities,
B: a grid of approximately 1400 elements, and returning
C: equipotential lines (force field), and
D: flowlines (flow field).

Modelling Variable Density Flow

Next we will consider the Münchehagen mathematical model of variable density flow with supporting field data (Weyer, 2006). The model was calculated along the cross-section A-B in Figure 3 which also shows the position of Borehole 226 whose water levels and chemistry are shown in Figure 4. The water levels and chemistry show downward flow of fresh groundwater to a depth of about 50 m, while upward flow of saline groundwater is indicated from below 50 m depth. The salinity of the salty ground-water is equivalent to ocean water. These data originate from Gronemeier et al. (1990).

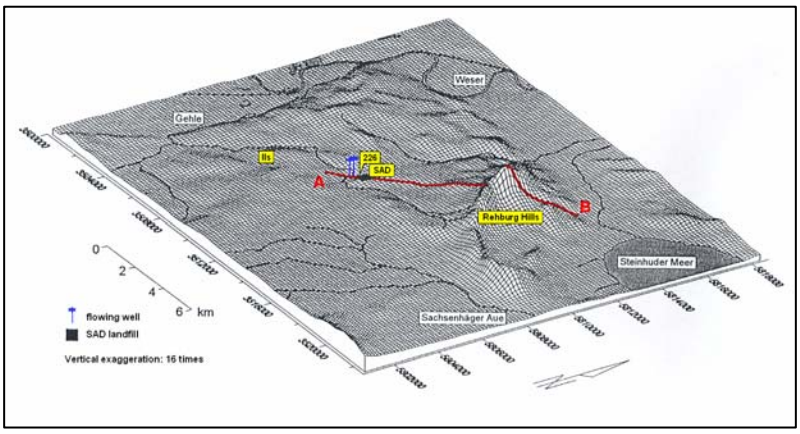

Fig. 3 Digital Elevation Model [DEM] of the area of the landfill Münchehagen [SAD] (after Weyer, 1996, 2006)

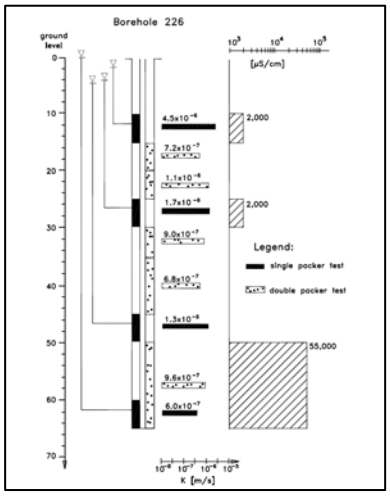

Fig. 4 Occurrence of electrical conductivity equivalent to ocean-type water at a depth of about 50 m in borehole 226 (Gronemeier et al, 1990, Figure 7)

The singular-run simulation of groundwater flow in the above cross-section (Fig. 5) was based on geologic data (Fig. 5A) from a public 1:25,000 map and rough estimations of contrast permeabilities. The position of the groundwater table followed the topography. The resultant

flow lines (Fig. 5C) went to depth of 900 to 1000 m, penetrating marl with evaporitic components. Figure 6 shows the same flow lines in a vertical exaggeration of 30:1. It shows that the flow lines of saline water reach a depth of 50 m before they turn laterally to the river Ils.

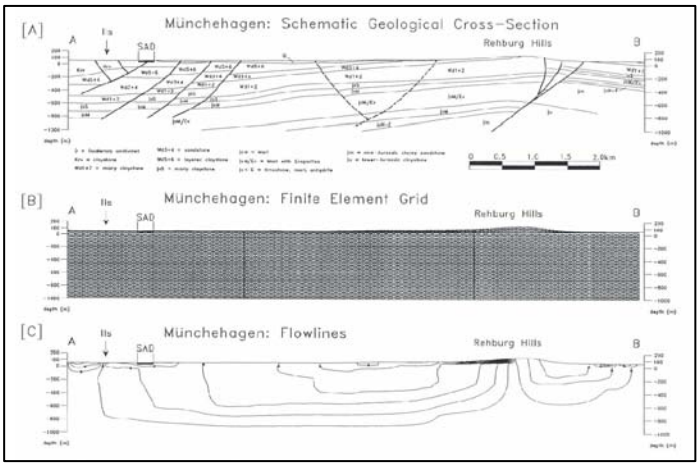

Fig. 5 2D-vertical model of groundwater flow directions in cross-section A-B in the Münchehagen landfill area (after Weyer, 1996, 2006).

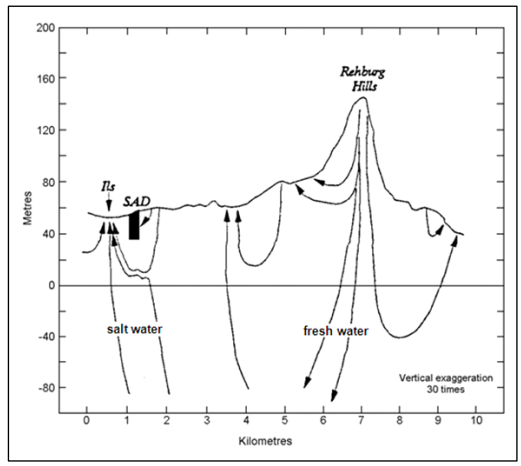

Fig. 6 Cross-section A-B showing flow lines calculated by 2D-vertical mathematical model; vertical exaggeration 30:1; SAD = landfill Münchehagen (after Weyer, 1996, 2006).

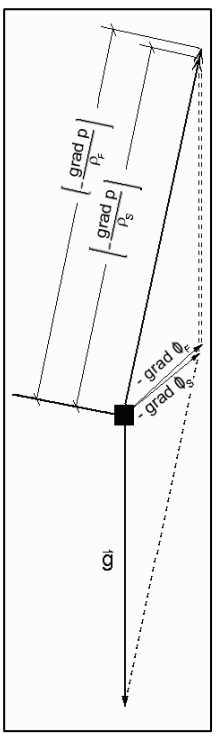

Fig. 7

Similarity in flow directions between fresh water and ocean-type (conductivity 55,000 µS/cm; TDS about 35,000 ppm) salt water (after Weyer, 1996, 2006b).

Thus, the model confirmed the field data (Fig. 4) as the field data confirmed the model. As a by-product, it has been established that variable density flow can be modelled with fresh water flow models. The reason for this is shown in Figure 7. As ocean water has a density of approximately 1.03 g/cm^3, the vectoral addition of the gravitational force (g) with the pressure potential force ($-1/\rho \cdot \text{grad } p$) returns similar directions and magnitudes for the force vector ($-\text{grad } \Phi$) for both fresh and ocean-type salt water.

Groundwater Flow in Aquitard Versus Flow in Underlying Aquifer

Freeze and Witherspoon (1967) showed that under undisturbed conditions, as shown here in Figure 8, approximately twice as much water flows through the overlying aquitard (downwards and upwards) as through the aquifer (laterally only). This result apparently contradicts common wisdom which assumes that most of the groundwater flow is confined to aquifers. The fact that this is not the case has important implications for the storage of CO_2 in saline aquifers and in reservoirs.

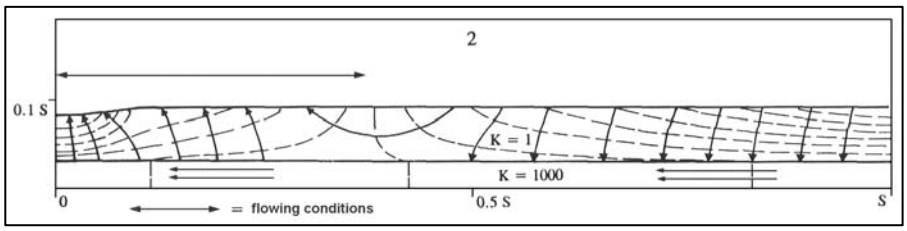

Fig. 8

Mathematical model by Freeze and Witherspoon (1967): Effect of buried higher-permeable layer upon groundwater flow pattern. Approximately twice as much water flows through the aquitard as through the aquifer.

How can we confirm the validity of that statement? It is actually simpler than one would assume at first sight. Figure 9 schematically depicts the flow situation and the piezometric heads in an aquifer overlain by an aquitard. The ground surface is taken as the groundwater table. The piezometric head line in the aquifer is a subdued replica of the groundwater table. In the recharge area, the piezometric head line is lower than the groundwater table; in the valleys the piezometric head line is higher than the groundwater table. A simple subtraction of the piezometric head line from the groundwater table will return positive values for the recharge area (with downward flow), and negative values for the discharge area (with upward flow).

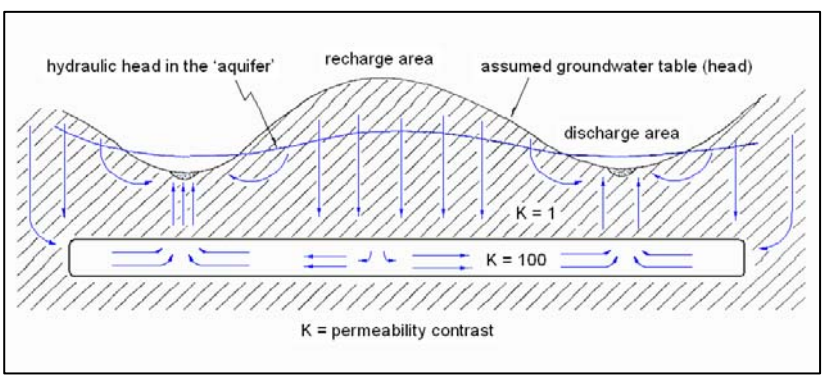

Fig. 9

Schematic diagram of groundwater flow with aquitard over a buried aquifer (after Weyer, 1996)

These conditions have been encountered world-wide. Here we show an example from the Loire area south of Orléans, France. There, in an area of about 8000 km^2, about 70 piezometers penetrated through the surface aquifer and through the aquitard into a deeper aquifer (the Cenoman Sands). Although there was only one piezometer per approximately 10 km^2 installed into the Cenoman Sands (Fig. 10), the subtraction of the head values in the Cenoman Aquifer from the groundwater table indicated clear recharge and discharge areas (hatched and yellow) following hills and valleys (Fig. 11). Thus the physical causality of flow through aquitards has been confirmed. How can this be explained?

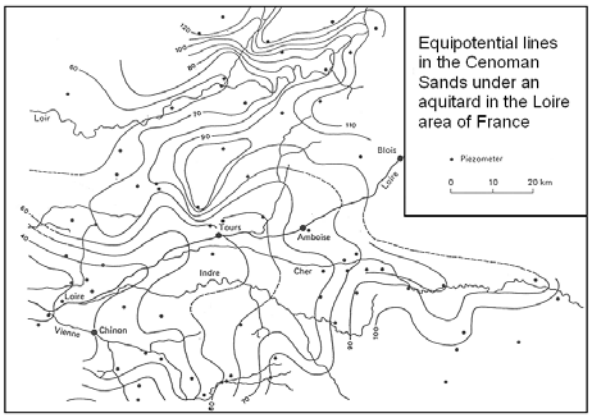

Fig. 10 Plan view of equipotential lines in a regional aquifer buried under an aquitard (after Albinet & Cottez, 1969)

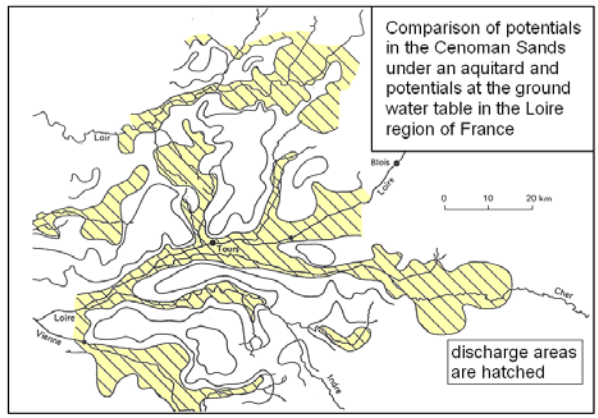

Fig. 11 Plan view of groundwater flow systems penetrating an aquitard (after Albinet & Cottez, 1969)

Under natural conditions, as shown in Figures 8 and 9, it is necessary that at any point the amount leaving the aquitard must equal that entering the aquifer and vice versa. That means that at this point, the Darcy equation (Hubbert, 1940, 1957) applies to the flow in both the aquitard and the aquifer. The flow volume (q) entering or leaving the aquifer is given by:

$$q = -\text{grad}\,\Phi \times A \times \sigma$$
$$= \text{hydraulic force} \times \text{area} \times \text{fluid conductivity}$$

As the flow leaving aquitard at its base is equal to the amount entering the aquifer at the top, the following balancing inequalities exist:

(1) $\sigma_{aquitard} << \sigma_{aquifer}$

(2) $A_{aquitard} >> A_{aquifer}$

(3) $\text{grad}\,\Phi_{aquitard} >> \text{grad}\,\Phi_{aquifer}$

Unbalanced flow across the boundary between the two would lead to an accumulation of water between the two layers which is a physical impossibility. To reduce energy consumption within the aquitard the flow directions are often near normal to the aquitard.

Conclusions

- Singular model runs in 2D-vertical modelling of groundwater flow in geological cross-sections with rough estimations of contrast permeabilities is suited to determine the general flow pattern and depth of groundwater flow systems.
- The same technique was applied to successfully determine the flow lines of regional variable density groundwater flow, as confirmed by field data.
- Contrary to widespread opinion that saline water with a density of 1.03 g/cm^3 would sink to the bottom of the geologic system, the saline water at the Münchehagen site flowed upwards from a depth of about 1 km and discharged into the river Ils.
- Approximately twice as much groundwater was shown to flow through the aquitard as compared to the aquifer.

References

Albinet, M., and S. Cottez, 1969. Utilisation et interprétation des cartes de différences de pression entre nappes superposés. Chronique d'Hydrogéologie, Nr. 12, S.43–48, B.R.G.M., [Paris] Orléans

Freeze, R.A. and P.A. Witherspoon, 1967. Theoretical analysis of regional groundwater flow: 2. Effect of water table configuration and subsurface permeability variation. Water Resources Research, vol.4, no.3, p. 581-590.

Gronemeier, K., H. Hammer, and J. Maier, 1990. Hydraulische und hydrodynamische Felduntersuchungen in klüftigen Sandsteinen für die geplante Sicherung einer Sonderabfalldeponie. Zeitschr. dt. geol. Ges., vol.141, p. 281-293, Hannover

Hubbert, M. King, 1940. The theory of groundwater motion. J.Geol., vol.48, No.8, p.785-944.

Hubbert, M. King, 1957. Darcy's law and the field equations of the flow of underground fluids. Bulletin de l'Association d'Hydologie Scientifique, No. 5, 1957, p.24-59.

Weyer, K.U., 1996. Physics of groundwater flow and its application to the migration of dissolved contaminants [Darlegung und Anwendung der Dynamik von Grundwasserfließsystemen auf die Migration von gelösten Schadstoffen im Grundwasser]. Research report to the German Federal Environmental Office [Umweltbundesamt, Berlin]. 204 pages [available in German from http://www.wkc-consultants.com].

Weyer, K.U., 2006. Industrial waste disposal site Münchehagen: Confinement of dissolved contaminants by discharging saline water. Revised version of paper originally submitted to Solutions '95, Congress of International Association of Hydrogeologists, Edmonton, Alberta, Canada, June 4-10, 1995, 9 pages [available from http://www.wda-consultants.com].

Chapter 4

[Poster 3]

Buoyancy, Pressure Potential and *Buoyancy Reversal*

K. Udo Weyer
WDA Consultants Inc., Calgary, AB, Canada
weyer@wda-consultants.com

Introduction

'Buoyancy forces' play a central role in the modelling of carbon sequestration, be it in the currently-applied methods to determine flow directions, or to determine the height of breakthrough columns for CO2. Usually 'buoyancy forces' are assumed to be directed vertically upwards or downwards, and their magnitudes are determined by density differences.

The general assumption is that fluids lighter than water (such as hydrocarbons and CO2) will rise vertically upwards and fluids heavier than water will sink to the bottom of the geologic layer packet. These opinions are based on the assumption of hydrostatic conditions (no-flow conditions) at sequestration sites. In reality, onshore sequestration sites (i.e. Weyburn, Ketzin, etc.) have fluids flowing under hydrodynamic conditions. Offshore injection sites (Sleipner, Snøhvit, etc.) are subject to hydrostatic conditions. Offshore sites close to shore may be totally subject to either condition.

Hubbert (1953) showed the basic difference between hydrostatic conditions and hydrodynamic ones (Fig. 1). In the hydrostatic case the gravitational force and the pressure potential force are of exactly the same magnitude but pointing in opposite directions. The resultant force (E in Hubbert's terminology; '–grad Φ' in this poster's terminology) is zero and no flow occurs. In the general hydrodynamic case the gravitational force and the pressure potential force do not assume opposite directions and equal magnitude. Therefore the resultant force vector is unequal to zero and flow occurs. In this case the 'buoyancy force' is not directed vertically upwards but can assume any direction in space including downward, as its direction follows that of the pressure potential force ($-1/\rho \cdot \text{grad } p$). In fact, the so-called 'buoyancy force' is the pressure potential force for the density of the fluid considered.

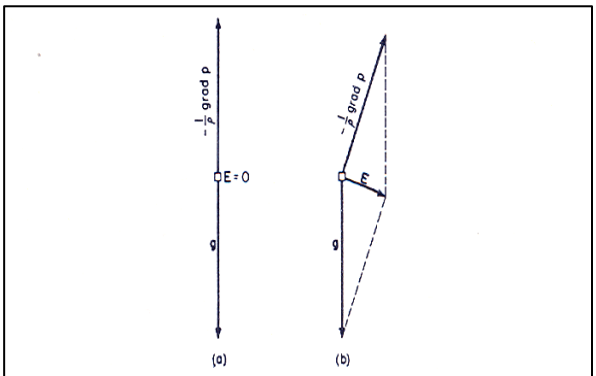

FIG. 4.—Physical interpretation of force-intensity vector **E**. (*a*) Hydrostatic case **E**=0; (*b*) hydrodynamic case.

Fig . 1 Hydrostatic forces versus hydrodynamic forces (taken from Hubbert, 1953).

Please note that low velocities and/or low amounts of flow are irrelevant for the determination of hydrostatic conditions. The direction of the so-called 'buoyancy force' is determined by the force field, not by the flow field. In a low-permeable environment, at any point the flow of groundwater may be slow and of minor amounts, but the associated pressure potential forces will be high and will determine the direction of the 'buoyancy forces'.

Hubbert, 1953, p.1960 showed that force potentials (energy / unit mass) of fresh groundwater determine the subsurface flow behaviours of other fluids such as salt water, oil, or gas (including CO_2 in liquid or gaseous form).

'Buoyancy forces' under Hydrostatic Conditions

Next we consider a hydrostatic condition within a freshwater body at the surface. Fig. 2 schematically shows the different pressure potential gradients (forces) for salt water, fresh water, oil, and gas.

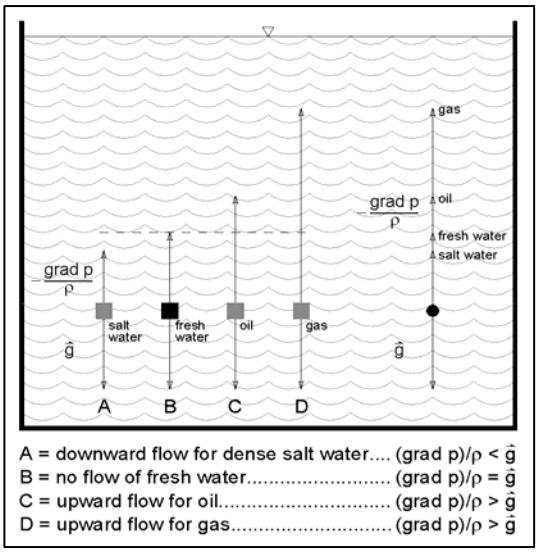

The combined force vectors on the right side of Fig. 2 amalgamate the pressure potential forces of fresh water, salt water, oil, and gas. They are all directed vertically upwards because the fresh water pressure potential force is directed vertically upwards. The direction of the fresh water pressure potential force determines the direction of the pressure potential forces for oil, gas and salt water. That is the reason why oil and gas float vertically upwards and saltwater vertically downward **under hydrostatic conditions**.

Fig. 2 Schematic derivation of pressure potential forces ('buoyancy forces') for oil, gas, and salt water under hydrostatic conditions

'Buoyancy forces' under Hydrodynamic Conditions

The above principles also apply under hydrodynamic flow conditions, except that the direction of the fresh water pressure potential force usually takes an oblique, non-vertical direction in space (Fig. 3). This is the key observation for comprehending the behaviour of so-called 'buoyancy forces' under hydrodynamic conditions.

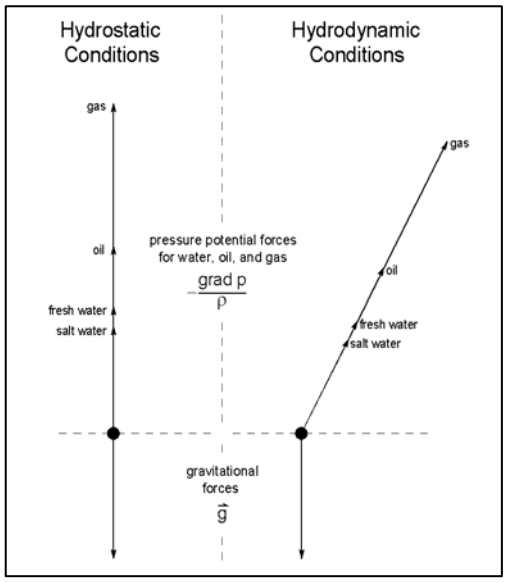

Fig. 3 Comparison of the direction of pressure potential forces (so-called 'buoyancy forces') under hydrostatic and hydrodynamic conditions

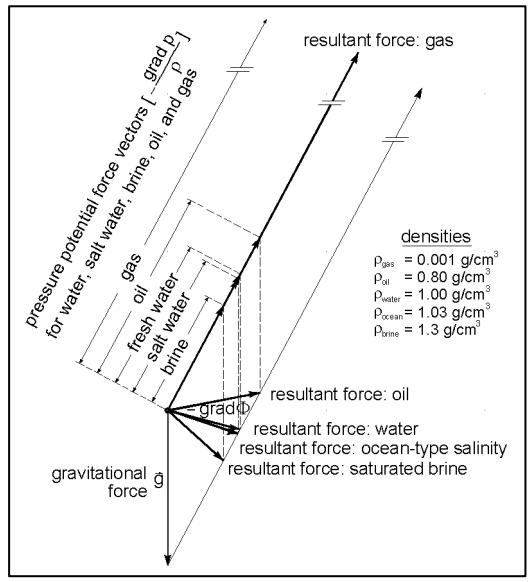

Fig. 4 Determination of differing flow directions for fresh water, ocean-type salt water, saturated brine, oil, and gas within the same fresh water force field (schematic diagram modified from Hubbert, 1953). The flow direction of supercritical CO_2 would be similar to that of oil, according to its density.

Fig. 4 shows the differing flow directions of various fluids within the fresh groundwater force field, as determined by vectoral addition. The different -grad Φ directions indicate the different flow directions for the fluids with different density in the same fresh groundwater force field. As a consequence, <u>the so-called vertically-upward (density $\rho < 1$ g/cm^3) and downward ($\rho > 1$ g/cm^3) directed 'buoyancy forces' do not exist under hydrodynamic conditions.</u>

The following photographs show upward-flowing salt water (Fig. 5) and saturated brine (Fig. 6) demonstrating that denser fluids can discharge at the surface.

Fig. 5 Discharging salt water from open borehole on south shore of Great Slave Lake, NWT, Canada (picture: Weyer, 1977)

Fig. 6 Upward discharge of saturated brine near Ft. Smith, NWT, Canada (picture: Weyer, 1977)

Buoyancy Reversal

Buoyancy Reversal was postulated by Weyer (1978) for the conditions of strong downward flow through low-permeable layers. In such a case, the pressure can decrease with depth (Fig. 7). These conditions occur when energy has to be taken from the compressed fluid element (groundwater) to maintain the amount of flow through low-permeable layers (aquitards), thus causing reduction in pressure with depth.

Hitchon et al. (1989) described those conditions for the Clearwater-Wilrich Aquitard in the Swan Hills region of Alberta, Canada (Fig. 8, 9). Fig. 10 shows the sequence of layers containing the Clearwater-Wilrich Aquitard with high-permeable layers below this particular aquitard. The occurrence of layers with *Buoyancy Reversal* is widespread and well-known within the oil industry, but explained differently.

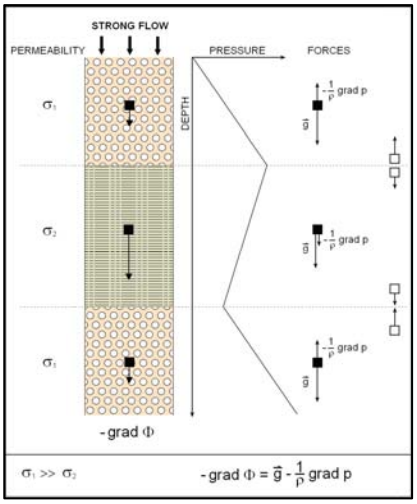

Fig. 7 Distribution of forces at *Buoyancy Reversal*

-grad Φ = hydraulic force

$-\vec{g}$ = gravitational force

$-1/\rho \bullet$ grad p = pressure potential force

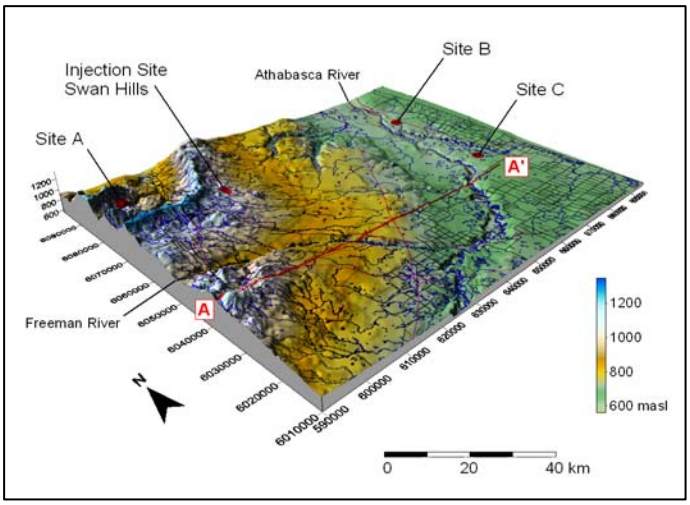

Fig. 8 Digital Elevation Model [DEM] of the Swan Hills area. The geologic cross-section A-A' (in Fig. 10) is marked as a red line. At the sites A, B, and C the occurrence of *Buoyancy Reversal* was measured within the Clearwater-Wilrich aquitard.

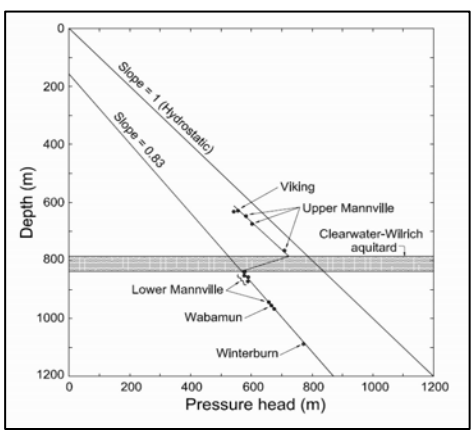

Fig. 9 *Buoyancy Reversal* at Site A within the Clearwater-Wilrich Aquitard (after Hitchon et al, 1989).

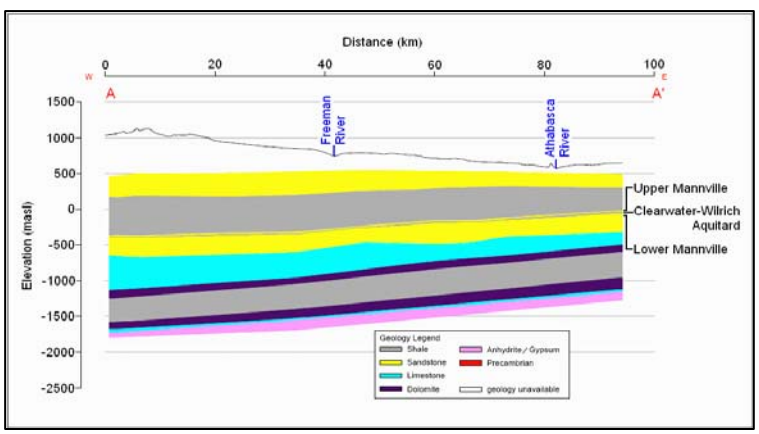

Fig. 10 Geologic cross-section A-A'. See Fig. 8 for location of cross-section.

Conclusions

- Under discharge areas, non-vertical pressure potential forces allow increased column length with respect to CCS breakthrough of aquitards by overcoming capillary forces.
- Under recharge areas with downward groundwater flow, aquitards with *Buoyancy Reversal* offer an additional defence against leakage of injected CO_2. While capillary forces are limited to the border between high- and low-permeable layers, the defence by *Buoyancy Reversal* is present throughout the low-permeable layer.

References

Hitchon, B, C.M. Sauveplane, S. Bachu, E.H. Koster, and A.T. Lytviak, 1989. Hydrogeology of the Swan Hills Area, Alberta: Evaluation for deep waste injection. Alberta Research Council Bulletin No. 58.

Hubbert, M. King, 1953. Entrapment of petroleum under hydrodynamic conditions. The Bulletin of the American Association of Petroleum Geologists, vol. 37, no. 8, August 1953.

Weyer, K.U., 1978. Hydraulic forces in permeable media. Mémoires du B.R.G.M., vol. 91, p.285-297, Orléans, France *[available from http://www.wda-consultants.com].*

Chapter 5

[Poster 4]

Trapping CO_2 by Means of Subsurface Water Flow (*Buoyancy Reversal*)

K. Udo Weyer
WDA Consultants Inc., Calgary, AB, Canada
weyer@wda-consultants.com

Introduction

Hubbert, 1953, p.1960 showed that the force potentials (energy / unit mass) of fresh groundwater and the derived force fields determine the subsurface flow behaviours of other fluids such as salt water, oil or gas (including CO_2 in liquid or gaseous form). That is the reason why the force fields of groundwater flow systems have a direct effect upon the migration behaviour of sequestered CO_2. The basic equations for the mechanical groundwater force fields are:

$$-\,grad\ \Phi = -\,grad\ \Phi_g - grad\ \Phi_p$$
$$-\,grad\ \Phi = \vec{g} - \frac{grad\ p}{\rho}$$

Adding the mechanical capillary forces (in this case for CO_2) expands the equation to:

$$-grad\ \Phi_{CO_2} = \vec{g} - \frac{grad\ P}{\rho_{CO_2}} - \frac{grad\ P_c}{\rho_{CO_2}}$$

fluid force | gravitational force | pressure potential force | capillary force

This poster concentrates, however, on non-capillary forces. Capillary forces occur only at borders between high- and low-permeable layers, while the other mechanical forces exist throughout the subsurface, including reservoirs, aquitards, caprocks, and saline aquifers. Therein lies the reason why groundwater flow occurs everywhere in the subsurface and flow systems are regional and continuous.

Modelling of Subsurface Fluid Flow

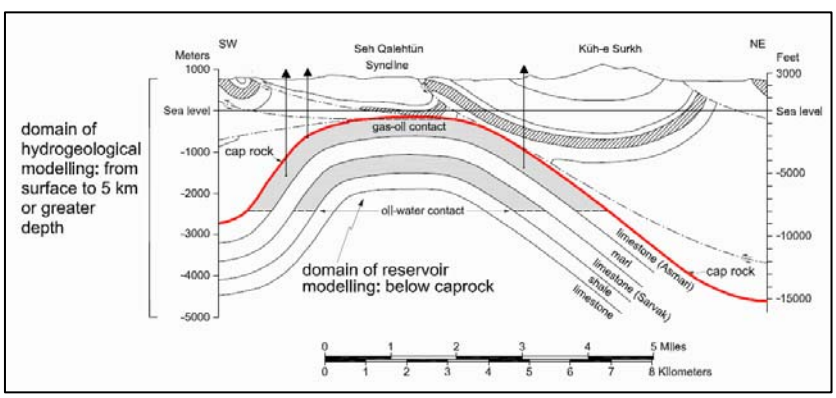

Fig. 1

SW-NE cross-section through the Gachsaran field with oil in the Asmari Formation and the Sarvak Formation in Iran. Figure modified after Dickey (1981, Fig.10-9) and Croft (2002).

Fig. 1 shows the limited range of reservoir simulators which take caprock as the upper boundary and deal with 'confined' flow only. Groundwater flow modelling, however, takes the groundwater table as the upper boundary and can calculate the force fields and groundwater flow to great depths, including through caprocks and reservoirs. As shown above, these groundwater force fields, under natural conditions, determine the migration behaviour of all other fluids in the subsurface. "*CO_2 injection involves dominantly hydrogeological (single-phase flow) processes in much of the reservoir and surrounding adjacent strata, with additional two-phase flow effects around the CO_2 plume itself*." [Chadwick et al., 2009]

"[A] *sand-shale boundary* [is] *an impermeable barrier to oil trapped in the sand, but not an impermeable barrier to the passage of water in either direction*" [Hubbert, 1953, p.1979]. If pressure (i.e. pressure gradient) is applied to the oil [CO_2] in the sand greater than the opposing capillary pressure (gradient) against the oil in the shale, oil [CO_2] will penetrate the shale. Fig. 2 shows downward-directed water flow penetrating the caprock and the hydrocarbon accumulation in a reservoir. While this phenomenon cannot be modelled by the widely-used reservoir simulators, it can be modelled by advanced hydrogeological modelling software.

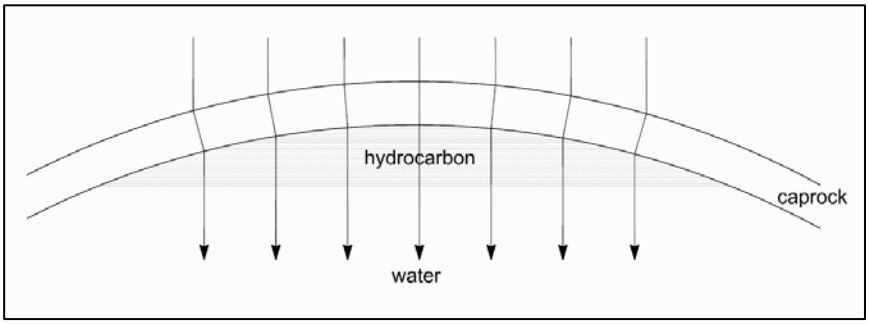

Fig. 2

Schematic of downward-directed water flow penetrating hydrocarbon accumulation and caprock. Due to capillary forces, hydrocarbons normally do not penetrate caprock while water does in either direction (upwards or downwards).

With respect to strong downward flow through caprock and aquitards, Weyer (1978) postulated the occurrence of downward-directed pressure potential forces ('buoyancy' forces) which he termed *Buoyancy Reversal*.

Buoyancy Reversal

Buoyancy Reversal can occur under conditions of strong downward flow through low-permeable layers. In such a case, the pressure can decrease with depth (Fig. 3) as energy is taken from the compressed fluid element (pressure potential) to maintain the amount of flow, thus causing reductions in pressure and a downward-directed pressure potential force or 'buoyancy' force (Weyer, 2009). Under downward flow conditions, *Buoyancy Reversal* occurs when -grad Φ > 9.81 m/s^2.

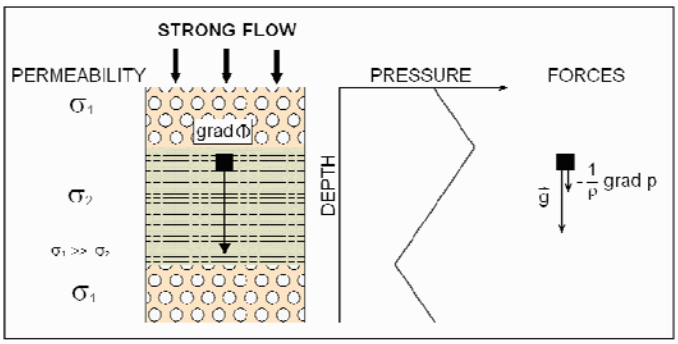

Fig. 3

Distribution of forces at *Buoyancy Reversal* (modified from Weyer, 2009)

-grad Φ = resultant hydraulic force
$-\vec{g}$ = gravitational force
-1/ρ · grad p = pressure potential force

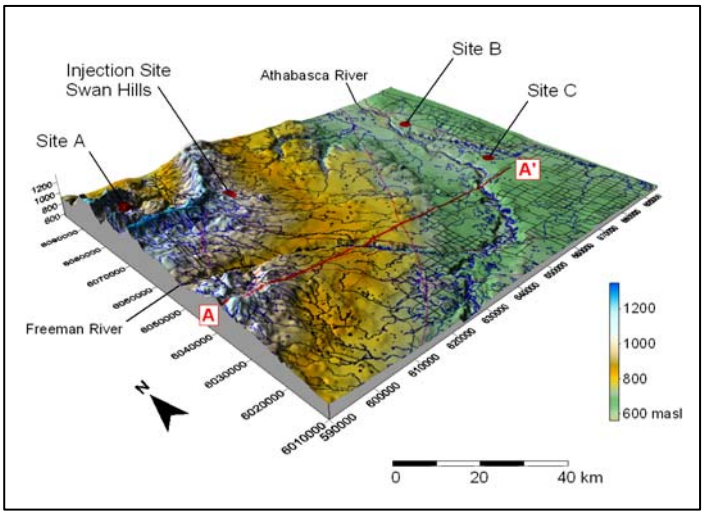

Fig. 4 Digital Elevation Model [DEM] of the Swan Hills area, Alberta, Canada. The geologic cross-section A-A' is marked as a red line (see Fig. 6). At the sites A, B, and C the occurrence of *Buoyancy Reversal* was measured within the Clearwater-Wilrich aquitard by Hitchon.et al. (1989).

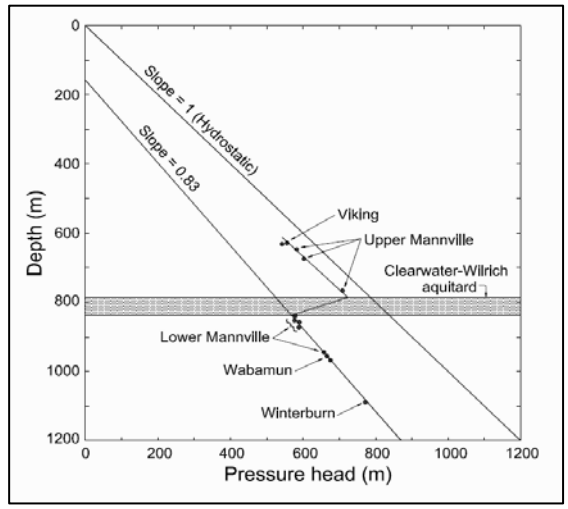

Fig. 5 *Buoyancy Reversal* at Site A within the Clearwater-Wilrich Aquitard (after Hitchon et al, 1989).

Hitchon et al. (1989) described those conditions for the Clearwater-Wilrich Aquitard in the Swan Hills region of Alberta, Canada (Fig. 4, 5). Fig. 6 shows the sequence of layers containing the Clearwater-Wilrich Aquitard with high-permeable layers below this particular aquitard. The occurrence of layers with *Buoyancy Reversal* is widespread and well-known within the oil industry, but explained differently.

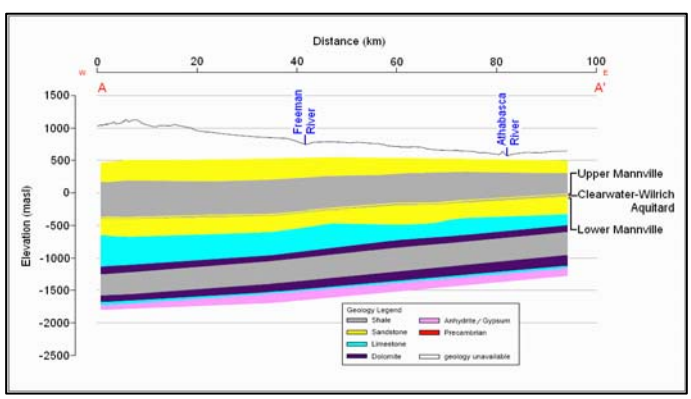

Fig. 6

Geologic cross-section A-A'. See Fig. 4 for location of cross-section.

The conditions giving rise to *Buoyancy Reversal* are usually created by downward flow from recharge areas through aquitards into high-permeable layers at depth. In the case of Swan Hills, the area with pronounced downward flow seemingly exceeds 10,000 km^2 as evidenced by sites A, B, and C in Fig. 4. In general, areas with deep downward flow are much larger than discharge areas with upward flow from depth.

Due to the downward-directed pressure potential force ($-1/\rho \cdot$ grad p), layers with *Buoyancy Reversal* act as an additional line of defence against leakage of CO_2. While capillary forces are limited to the border between high- and low-permeable layers, the defence by *Buoyancy Reversal* is present throughout the low-permeable layer.

Effects of Oil Production and CO_2 Injection Upon Fluid Flow

Within an operating reservoir, hydraulic sink conditions are created (Fig. 7) and any *Buoyancy Reversal* present would be enhanced or possibly newly created because of reduction of fluid potential in the reservoir.

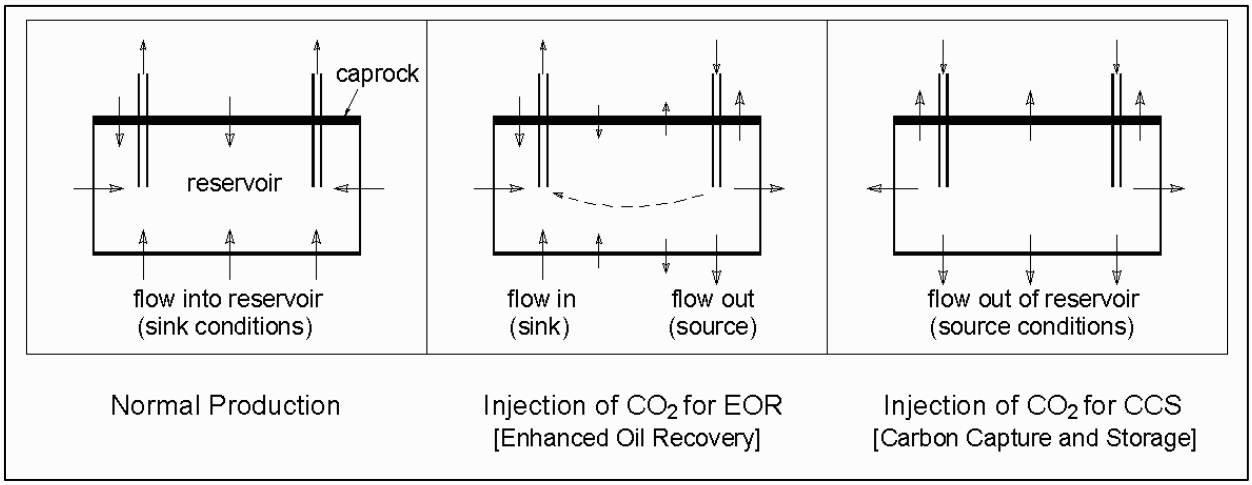

Fig. 7 Changes of sink towards source conditions within a reservoir during petroleum production, EOR and subsequent CCS.

As EOR and carbon storage begin injecting CO_2 at high pressures into the reservoir, the sink conditions shift towards source conditions (Fig. 7). These source conditions would propel water in all directions away from the injection point(s), and thereby potentially eradicate any *Buoyancy Reversal* present.

There exists, however, a way to maintain *Buoyancy Reversal* parallel to the injection of CO_2 if the situation warrants it. It would mean to pump water from greater depths within the CO_2 injection layer or beneath it, and subsequently re-inject it above the caprock (Fig. 8), if the water chemistry allows this. Water could also be taken from layers with more favourable chemistry. It is recommended that appropriate field studies be undertaken and that head and pressure be routinely measured above caprocks at planned and operating carbon storage sites.

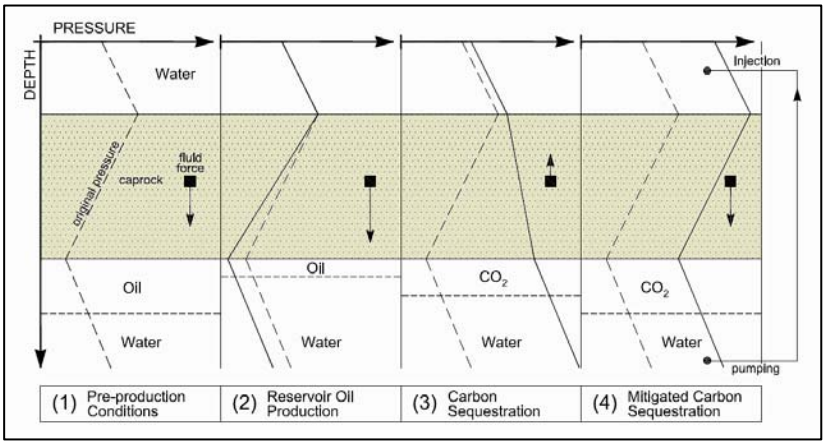

Fig. 8

Schematic pressure-depth relationship at (1) a natural occurrence of *Buoyancy Reversal*, and subsequent pressure pattern during (2) oil production, (3) carbon sequestration, and (4) mitigation of *Buoyancy Reversal* through pumping water from beneath the CO_2 layer (or other sources) and injecting it above the caprock.

During injection itself, the behaviour of CO_2 at the injection site is mainly affected by the high injection pressure and gradients at that location although the gravitational forces exist there as well. The further CO_2 migrates from the wells, the more the groundwater force fields take control, albeit with increased pressure potential gradients due to the injection pressure. In general the additional pressure should decrease with the cube of the distance from the injection site, i.e. by a factor of 10^{-9} at about one kilometer distance from the injection site. Hence, although the natural force fields are modified by the introduction of a new source area, much of the flow will, in the end, still be directed towards the major regional groundwater discharge areas established under natural conditions in dependence of the topography of the groundwater table.

Conclusions

- For the modelling of CO_2 migration at storage sites, the use of reservoir simulators should be discontinued and replaced with advanced hydrogeologic modelling techniques. To achieve reliable results and leakage forecasts Hubbert's methodology needs to be merged with parts of the methodology of reservoir engineering.
- Groundwater flow penetrates caprock and aquitards.
- The occurrence of *Buoyancy Reversal* is widespread in aquitards under elevated areas and may be used for further protection in CO_2 storage, in addition to capillary forces.
- Loss of *Buoyancy Reversal* could be countermanded by pumping water from below the CO_2 storage (or other sources) and injecting it above the caprock.

References

Chadwick, R.A., D.J. Noy, and S. Holloway, 2009. Flow processes and pressure evolution in aquifers during the injection of supercritical CO2 as a greenhouse gas mitigation measure. Petroleum Geosci., vol. 15, p.59-73.

Croft, G.D., 2002. Oil Fields of the Gulf region : An illustrated atlas. Published by Greg Croft Inc., March, 2002

Dickey, P.A., 1981. Petroleum Development Geology. 2nd edition, PennWell Books

Hitchon, B, C.M. Sauveplane, S. Bachu, E.H. Koster, and A.T. Lytviak, 1989. Hydrogeology of the Swan Hills Area, Alberta: Evaluation for deep waste injection. ARC Bulletin No. 58.

Hubbert, M. King, 1953. Entrapment of petroleum under hydrodynamic conditions. The Bulletin of the American Association of Petroleum Geologists, vol. 37, no. 8, p.1954-2026.

Weyer, K.U., 1978. Hydraulic forces in permeable media. Mémoires du B.R.G.M., vol. 91, p.285-297, Orléans, France [available from http://www.wda-consultants.com].

Weyer, K.U., 2009. Buoyancy, Pressure Potential and *Buoyancy Reversal*. Poster Presentation at SEG 2009 Summer Research Workshop, CO_2 Sequestration Geophysics, 23-27 August, 2009, Banff, Canada, Abstract Book, 4 pages.

Chapter 6

Conditions for the occurrence of *Buoyancy Reversal* [BR] in hydraulic force fields with downward-directed flow through aquitards (caprocks)

K. Udo Weyer and James C. Ellis
WDA Consultants Inc., Calgary, AB, Canada
weyer@wda-consultants.com

The physical and hydrogeological conditions for the occurrence of *Buoyancy Reversal* (Weyer, 1978) have been outlined above in chapters 4 and 5. This chapter attaches numbers to those conditions to facilitate field recognition and practical application of *Buoyancy Reversal* [BR].

The calculation of these numbers is based on Hubbert's Force Potential (Hubbert, 1940) and on the summary tables provided by Weyer (1978, 1996). The application of the gravitational and pressure potential force fields (Hubbert, 1940) allows the calculation of the hydraulic gradient (-grad Φ) in regions of vertically downward-directed flow above which *Buoyancy Reversal* [BR] with associated decrease of pressure potential occurs with increasing depth (Weyer, 2009). Below this gradient threshold, the pressure potential increases with depth under vertically downward-directed flow conditions. For fresh water at a temperature of 20°C and related density and viscosity that threshold value is -grad Φ = 9.81 m/s^2

-grad Φ < 9.81 m/s^2	pressure potential increases with depth
-grad Φ = 9.81 m/s^2	pressure potential does not change with depth
-grad Φ > 9.81 m/s^2	pressure potential decreases with depth [BR]

In terms of head values (the freshwater level measured in piezometers), the threshold value for the head differences $\Delta h/\Delta l$ is 1 m/m.

$\Delta h/\Delta l$ < 1 m/m	pressure potential increases with depth
$\Delta h/\Delta l$ = 1 m/m	pressure potential does not change with depth
$\Delta h/\Delta l$ > 1 m/m	pressure potential decreases with depth [BR]

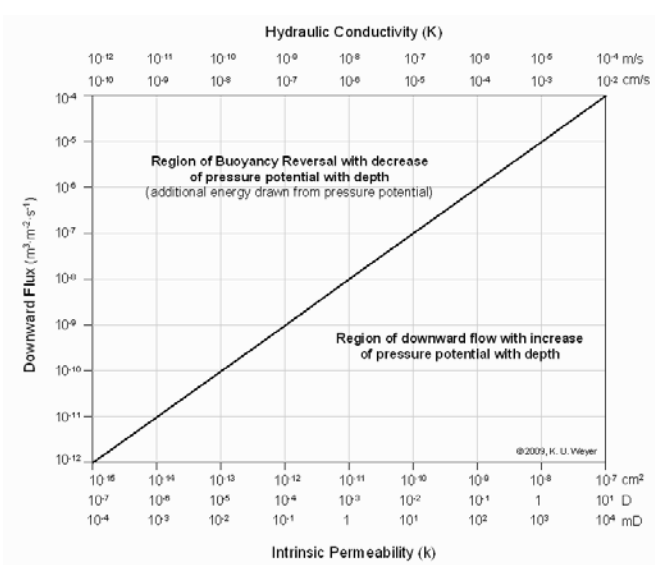

Fig. 1

Occurrence of *Buoyancy Reversal* [BR] in aquitards and caprocks under vertical downward flow of water at 20° C and density and viscosity of fresh groundwater.

Fig. 1 shows the threshold of the hydraulic gradient (-grad Φ) and the associated counterplay of flux and permeability. In the diagram the hydraulic gradient threshold occurs along the oblique line separating the area of decrease of pressure potential with depth [BR – *Buoyancy Reversal*, upper triangle] from the area of increase of pressure potential with depth (lower triangle). In aquitards with the threshold gradient -grad Φ = 9.81 m/s^2 (or $\Delta h/\Delta l$ = 1 m/m) the pressure potential does not change within the aquitard.

The subsurface appearance of *Buoyancy Reversal* is dependent on the energy gradient (-grad Φ) and Darcy's equation (written in field terms). Therefore, the occurrence of *Buoyancy Reversal* is dependent on the counterplay of flux and permeability as shown in Fig. 1. The higher the flux the higher the permeability corresponding to the threshold gradient and vice versa.

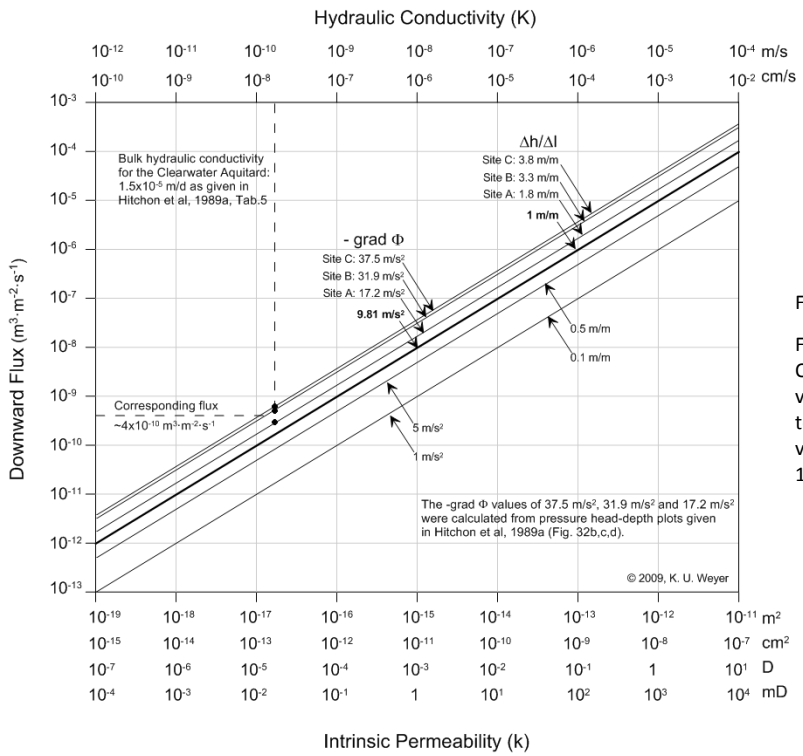

Fig. 2

Field example Clearwater- Wilrich aquitard: Occurrence of *Buoyancy Reversal* [BR] under vertical downward flow of freshwater assumed to be at 20° C and with the related density and viscosity. [Data extracted from Hitchon et al., 1989a]

Fig. 2 depicts field data extracted from Hitchon et al, 1989a for sites A, B, and C (for location see Fig. 3). In the diagram the respective gradients appear as straight lines marked with the hydraulic gradients and the corresponding head differences. The thick straight line marks the threshold gradient discussed above.

Hitchon et al. (1989a, Table 5) report the average permeability for the Clearwater-Wilrich aquitard to be 1.5x10^{-5} m/day (1.8x10^{-10} m/s; 1.8x10^{-5} D). Thereby the physical conditions at Sites A, B and C can be determined as the intersection between the straight gradient lines and the dotted vertical line indicating the average permeability of the Clearwater-Wilrich aquifer. The projection onto the y-axis determines the corresponding flux to be approximately 4x10^{-10} m^{3}m^{-2}s^{-1} (0.035 l per m^2 per day; 35 m^3 per km^2 per day).

Tab. 1 lists the field data used in Fig. 2, additional field data from Alberta and artificial data within the triangle of increased pressure potential with depth.

Source	Site ID / Location	Thickness of Aquitard [Δl] (m)	Pressure Head Difference (m)	Total Head Difference [Δh] (m)	Δh / Δl (m/m)	-grad Φ (m/s^2)
Pressure Potential Decreasing with Depth [BR]						
Hitchon et al., 1989a, Fig. 32b	Tp 64 R 1-2 W5M (Site A)	55	155	210	3.8	37.5
Hitchon et al., 1989a, Fig. 32c	Tp 67 R 2 W5M (Site B)	40	90	130	3.3	31.9
Hitchon et al., 1989a, Fig. 32d	Tp 68 R 10 W5M (Site C)	40	30	70	1.8	17.2
Bachu et al., 1993, Fig. 27b	16-36-71-24 W4M	120	56	176	1.5	14.4
Hitchon et al., 1989b, Fig. 51c	11-21-60-08 W4M	23	10	33	1.4	14.1
Pressure Potential Increasing with Depth						
Data assumed	no location	--	--	--	0.5	5
Data assumed	no location	--	--	--	0.1	1

Tab. 1 Observed and assumed hydraulic gradients at sites with pressure potentials decreasing with depth [*Buoyancy Reversal*] and with pressure potential increasing with depth. Gradient for Hitchon et al. 1989b taken as average value. Locations are approximate.

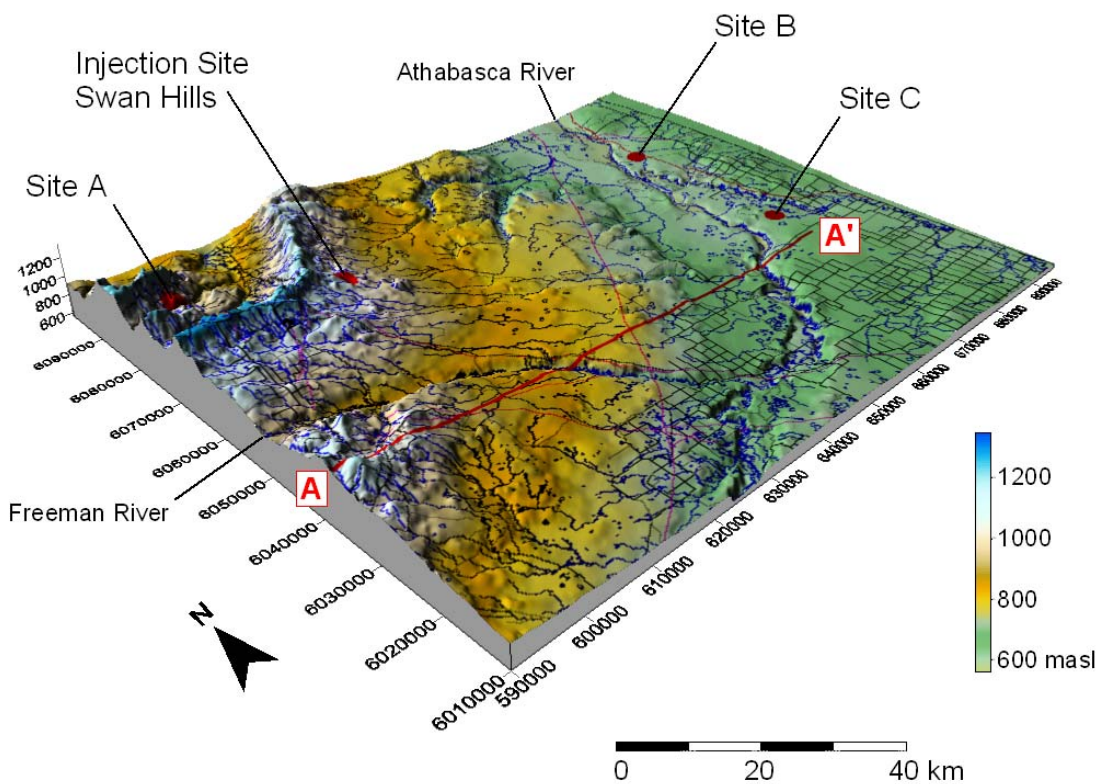

Fig. 3 Digital Elevation Model [DEM] of the Swan Hills area. The geologic cross-section A-A' (in Fig. 4) is marked as a red line. At the sites A, B, and C the occurrence of *Buoyancy Reversal* was measured within the Clearwater-Wilrich aquitard by Hitchon et al., 1989a.

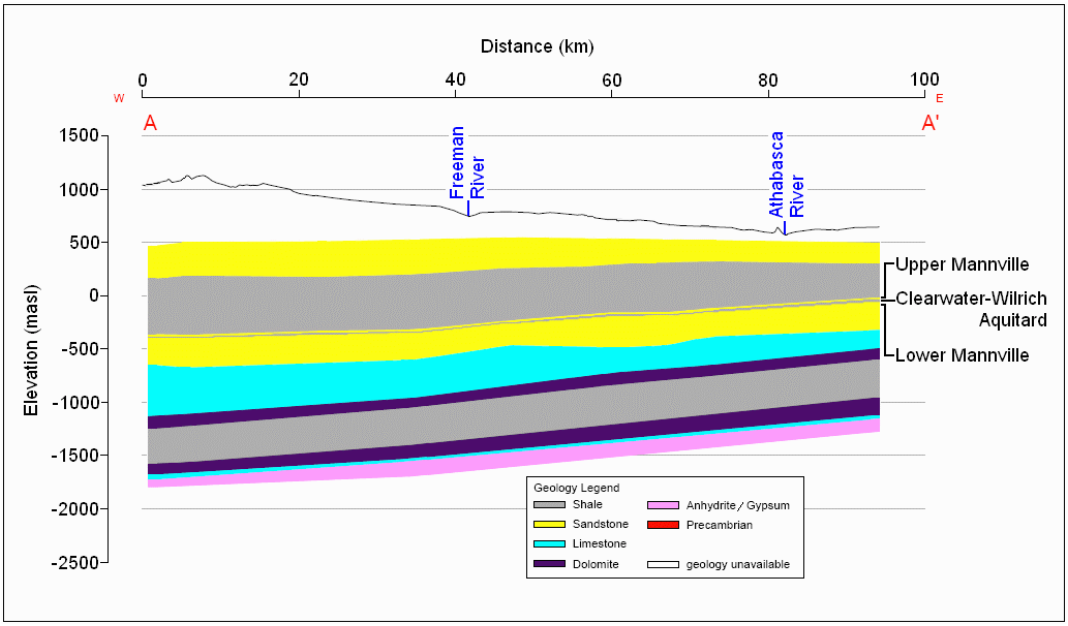

Fig. 4 Geologic cross-section A-A'. See Fig. 3 for location of cross-section.

Fig. 4 presents the general geology within the cross-section A-A'. The higher permeability of the limestone and dolomite layers underneath the Clearwater-Wilrich aquitard cause regional downward flow from the recharge area Swan Hills through the Clearwater-Wilrich aquitard into these layers due to the thermodynamic principle of minimizing the overall energy consumption. The natural discharge area is the valley of the Athabasca River.

References:

Bachu, S., J.R. Underschultz, B. Hitchon, and D. Cotterill, 1993. Regional-Scale Subsurface Hydrogeology in Northeast Alberta. Alberta Research Council, Bulletin No. 61.

Hitchon, B, C.M. Sauveplane, S. Bachu, E.H. Koster, and A.T. Lytviak, 1989a. Hydrogeology of the Swan Hills Area, Alberta: Evaluation for deep waste injection. Alberta Research Council, Bulletin No. 58 [*Dec 2009: available electronically at no charge from AGS-info@ERCB.ca*].

Hitchon, B, S. Bachu, C.M. Sauveplane, A. Ing, A.T. Lytviak, and J.R. Underschultz, 1989b. Hydrogeological and geothermal regimes in the Phanerozoic succession, Cold Lake area, Alberta and Saskatchewan. Alberta Research Council, Bulletin No. 59 [*Dec 2009: available electronically at no charge from AGS-info@ERCB.ca*].

Hubbert, M. King, 1940. The theory of groundwater motion. J.Geol., vol.48, No.8, p.785-944.

Weyer, K.U., 1978. Hydraulic forces in permeable media. Mémoires du B.R.G.M., vol. 91, p.285-297, Orléans, France [*available from http://www.wda-consultants.com*].

Weyer, K.U., 1996. Darlegung und Anwendung der Dynamik von Grundwasserfließsystemen auf die Migration von gelösten Schadstoffen im Grundwasser [Physics of groundwater flow and its application to the migration of dissolved contaminants]. Final Research report to the Federal Environmental Office of the German Government. 204 pages, 79 fig., 16 photographs, 15 tab. [in German]: April 1996 [*available from http://www.wkc-consultants.com*].

Weyer, K.U., 2009. Buoyancy, Pressure Potential and *Buoyancy Reversal*. Poster and Abstract SEG 2009, Summer Research Workshop: CO_2 Sequestration Geophysics, 23-27 Aug. 2009, Banff, Alberta, Canada.

Chapter 7

Off-shore versus on-shore geological storage of CO_2

K. Udo Weyer
WDA Consultants Inc., Calgary, AB, Canada
weyer@wda-consultants.com

The application of Hubbert's Force Potential, of the Theory of Gravitational Groundwater Flow Systems, and of the phenomenon of *Buoyancy Reversal* [BR] adds new dimensions to the subsurface trapping and geological storage of CO_2 . Firstly it leads to a division of fluid dynamics into off-shore and on-shore geological storage. Off-shore storage sites like Sleipner experience hydrostatic conditions and are therefore devoid of gravity-driven subsurface flow. Hence the traditional vertical buoyancy forces play a role as outlined in Ch. 4. A physically-correct force treatment would, however, make use of pressure potential gradients and not just pressure gradients.

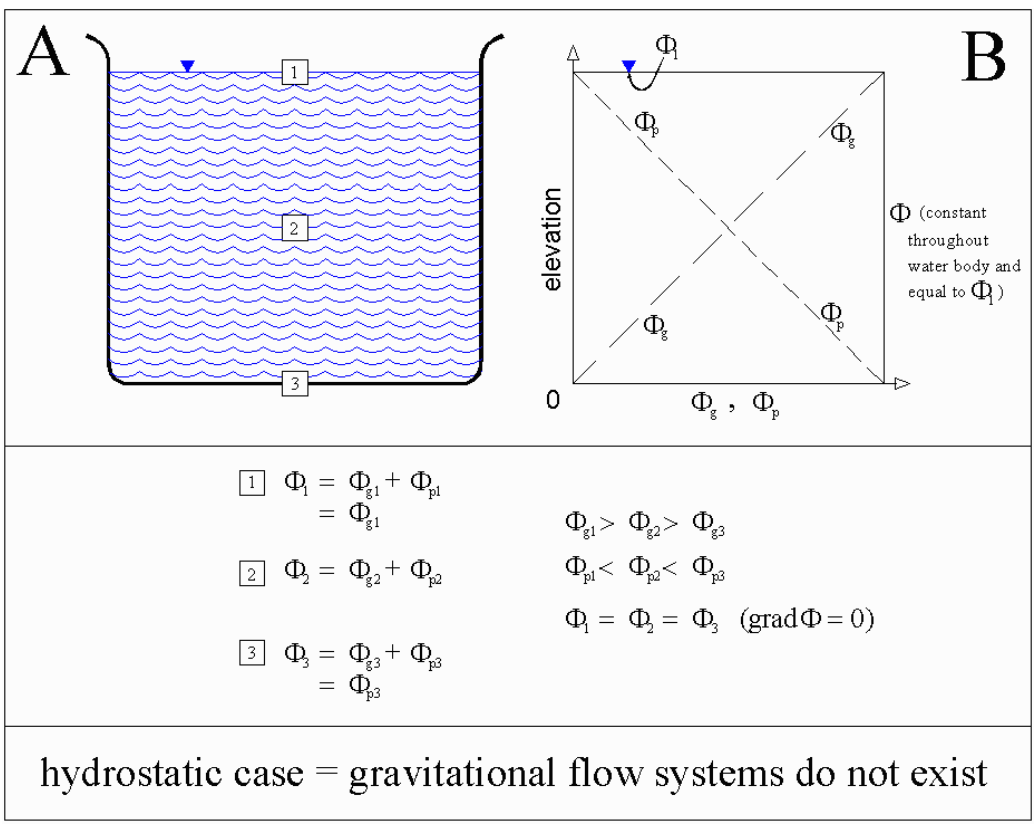

Fig. 1 Hydrostatic conditions in a pail. The value of the fluid potential ϕ is constant throughout the water body (part A) and determined by the surface elevation according to the equation $\phi = hg$ (Weyer, 1978) where h is the head and g the earth acceleration. The gravitational potential ϕ_g and the pressure potential ϕ_p , however, change in synchronous opposition with depth (part B) such that the gravitational potential ϕ_g decreases with depth (part B; line ϕ_g) at the same rate as the pressure potential ϕ_p (part B; line ϕ_p) increases with depth. Therefore the additions of the gravitational and pressure potential return the same hydraulic potential ϕ, namely that of the surface, at all positions within the water body in the pail. Within the hydrostatic water body, the gradient of the hydraulic potential is 0 (grad ϕ = 0) and no gravity-driven flow occurs.

Fig. 1 outlines the energy distribution in a hydrostatic water body, say a pail of water, a lake, or the sea. The hydraulic potential

$$\phi = \phi_g + \phi_p \qquad (1)$$

has the same magnitude at all positions within the waterbody (where ϕ_g would be the gravitational potential and ϕ_p the pressure potential; for more explanations see Weyer, 1978):

$$\phi_1 = \phi_2 = \phi_3 \qquad (2)$$

Given a constant density throughout, this would hold true within any surface water body and within subsurface water beneath the sea. The gravitational potential ϕ_g and the pressure potential ϕ_p are, however, conjoined such that their respective additions would always result in the magnitude of the total hydraulic potential ϕ equalling that of the surface , as in equation (2) above

$$\phi_{g1} > \phi_{g2} > \phi_{g3} \qquad (3)$$
$$\phi_{p1} < \phi_{p2} < \phi_{p3} \qquad (4)$$

As the hydraulic potential is the same anywhere within the hydrostatic water bodies. The hydraulic force gradient within a hydrostatic field is

$$-\text{grad}\ \phi = 0 \qquad (5)$$

and no gravity-driven water flow occurs. These conditions occur at all off-shore geological storage sites wherein injection of CO_2 causes buoyancy-driven (density-driven) flow within a system without gravity-driven flow. This process has been well documented under the North Sea at the Sleipner site. Other off-shore sites with similar characteristics are Snøhvit in the North Sea off the coast of Norway and the Pre-Salt targets within the Santos Basin and Campos Basin in the Atlantic off the coast of Brazil.

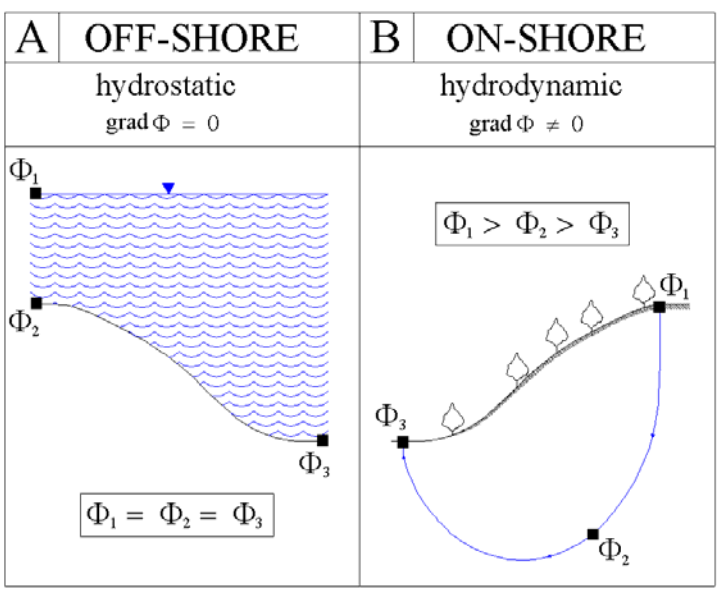

Fig. 2 Comparison of hydrostatic and hydrodynamic conditions in subsurface fluid flow.
Φ : hydraulic potential
-grad Φ : hydraulic force

Fig. 2 compares hydrostatic conditions at off-shore sites (Fig. 2A: grad $\phi = 0$) with hydrodynamic conditions at on-shore sites (Fig. 2B: grad $\phi \neq 0$). At the latter there exist the following inequalities

$$\phi_1 > \phi_2 > \phi_3 \qquad (6)$$

such that

$$-\text{grad}\ \phi \neq 0 \qquad (7)$$

and therefore gravitational groundwater flow systems exist. Under special geological conditions the discharge arm of on-shore flow systems may extend some distance under the coastal sea area and in bays.

The K12B project in the Netherlands and the Gorgon project in Australia are perceivably located within the border area of off-shore (hydrostatic flow regime) and on-shore (hydrodynamic flow regime) conditions and would need special investigations to determine the dominant gravitational flow regime. In general, one needs to determine which mechanical force fields and groundwater flow systems dominate the fluid flow at all selected injection sites, as caused by the boundary conditions.

At off-shore sites (i.e. Sleipner in the North Sea) the gravitational fluid flow system is hydrostatic (-grad $\Phi = 0$), whereas at on-shore sites the gravitational fluid flow systems are hydrodynamic (-grad $\Phi \neq 0$) and can exert a dominant effect on the migration of injected CO_2. Such on-shore sites include, but are not limited to, in North America: Weyburn (Saskatchewan), Zama, Wabamun, Alberta Saline Aquifer Project (ASAP), Heartland (all Alberta), Frio and others (Texas), Tea Pot Dome (Wyoming), and all seven DOE Regional Partnership projects in the USA; in Europe: Ketzin (Germany), Recopol (Poland), and Sulcis (Italy); in Africa, Australia, Asia and South America: In Salah (Algeria), Otway (Australia), Nagaoka (Japan), and Rio Pojuca (Brazil).

The lateral extent of groundwater flow systems reaches from a few meters to 500 km or more (as in the Gulf region, Australia, the USA, and elsewhere). The groundwater flow systems can penetrate to 5 or more kilometers in depth. Recharge areas of large scale groundwater flow systems (underpressured as compared to an assumed hydrostatic pressure) would lend themselves as target areas for geologic carbon storage while discharge areas (overpressured as compared to an assumed hydrostatic pressure) may be less desirable for large scale carbon storage. Trapping by *Buoyancy Reversal* occurs naturally under upland areas. It does not naturally occur, however, in discharge areas with deep-seated upward flow directions.

Chapters 2 and 3 concerned themselves with the basic physics and appearance of groundwater flow systems and contained more information on these systems. Chapter 4 described the effects of the force fields of fresh groundwater upon the migration of hydrocarbons and injected CO_2 towards and away from CO_2 traps.

At all on-shore project areas, gravitational groundwater flow systems will determine the long term migration path of injected CO_2. Only within the immediate neighbourhood of the injection site will the injection pressure be a major modifier of the gravitational groundwater flow

systems until the injection pressure dissipates. The long term migration behaviour of injected CO_2 will be determined by the natural force fields of the regional groundwater flow. Therein lies the reason why regional groundwater flow investigations need to be undertaken at all these sites using advanced hydrogeologic methodology. In addition hydrogeological mathematical model codes need to be adopted and applied to the determine the interference effects and magnitude of large scale CO_2 storage projects.

Weyer (1996, 2006a, 2006b) developed a set of tools to undertake such regional groundwater flow investiations based on available geological and topographical data as part of a research project for the German Umweltbundesamt (German Federal Office of Environment). These tools were successfully tested with field data from several sites. One of these test results has been described in Ch. 3 (Figs. 3 – 7). There, Fig. 3 shows that gravitational groundwater flow of variable density recharged on the 90 m high Rehburg Hills penetrated to a depth of approximately 1 km or more below ground surface (as evidenced by a selected set of flow lines) and subsequently rose to the River Ils despite an increased density of ~1.03 g/cm^3. In this field case fresh water modelling (density ρ = 1 g/cm^3) was adequate (as evidenced by field data) to simulate flow lines for variable density flow with a density increase from 1 to 1.03 g/cm^3, the density of sea water (for explanation, see Fig. 7 in Ch. 3).

Elevation differences between groundwater recharge and discharge areas as well as the geological structure (the vertical and lateral distribution of permeabilities) determine the pattern, the lateral extent, and penetration depth of groundwater flow systems. Below we give examples of the topography at three presently operating or planned CO_2 sequestration sites in Canada. The topographical elevation differences (as an indicator for the topographical pattern of the groundwater table) are an important determinant for the existance of large scale and deeply-penetrating gravitational groundwater flow system. The presence of these flow systems determines the long term migration behaviour of injected CO_2 .

The first example is the Weyburn EOR site south of Regina in Saskatchewan (Chalaturnyk and Durocher, 2006). Figs. 3, 4 and 5 show the topographic boundary conditions (i.e. approximate groundwater table) of the gravitational regional flow systems involved in the area of Weyburn, Saskatchewan, Canada. The second example is the Zama site in NW Alberta (Smith et al., 2007). Figs. 6, 7 and 8 show a DEM (Digital Elevation Model) and a topographical cross-section through the Zama project site and surrounding area. The third example is the Wabamun project (Keith and Lavoie, 2009). Figs. 9, 10 and 11 depict the DEM and a topographical cross-section for the Wabamun project site in Central Alberta.

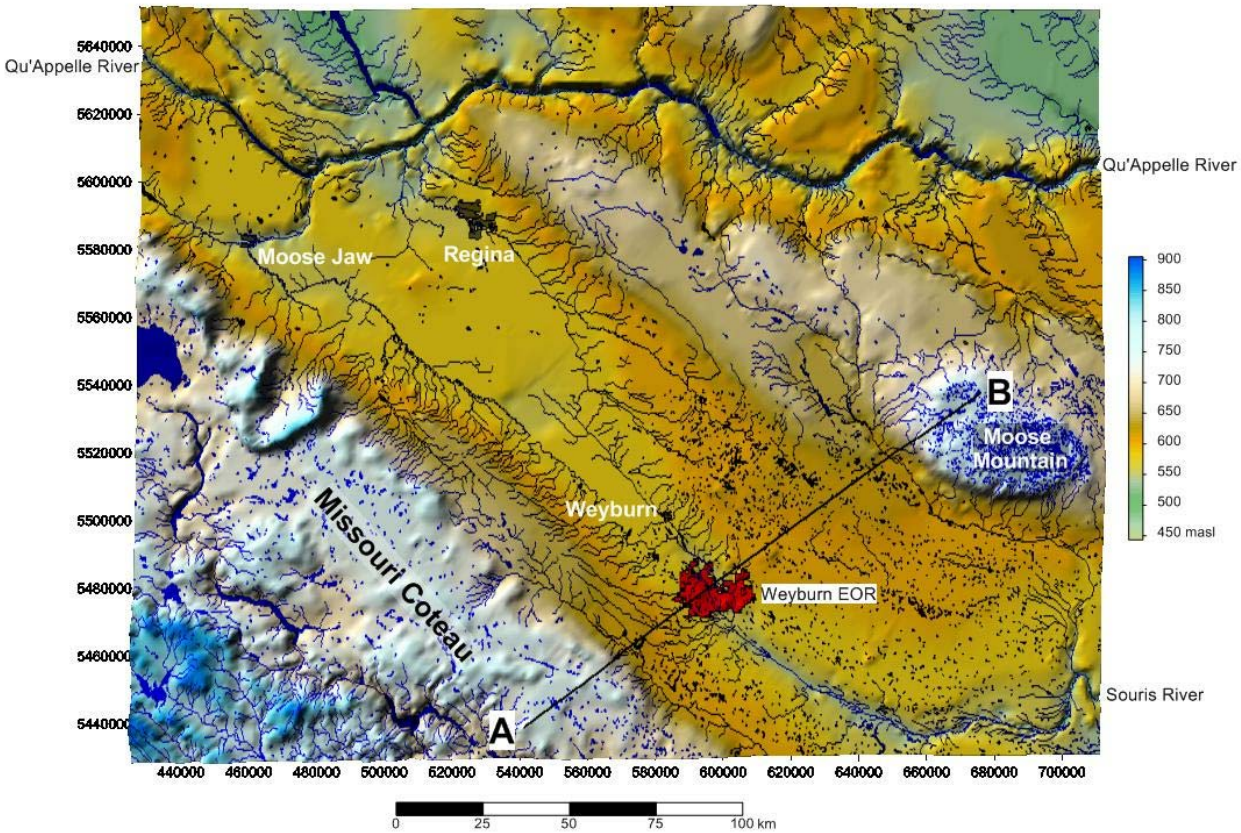

Fig. 3 Bird's-eye view of the DEM for the general Weyburn area based on NTDB 1:250,000 digital maps 062E (Weyburn), 062L (Melville), 072H (Willow Bunch Lake) and 072I (Regina). Topographical cross-section A-B is shown in Fig. 5.

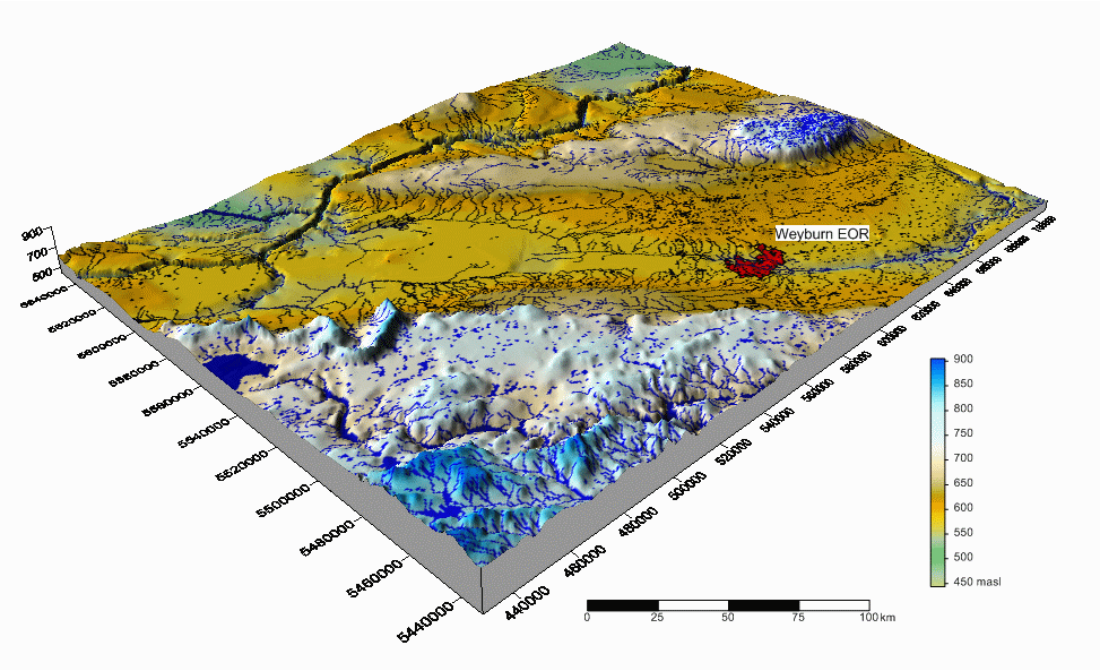

Fig. 4 Oblique view of the DEM for the general Weyburn area. Weyburn EOR is topographically located in a regional lowland (regional discharge area) flanked to the southwest by the Missouri Coteau and to the northeast by Moose Mountain and elevated surroundings (regional recharge areas).

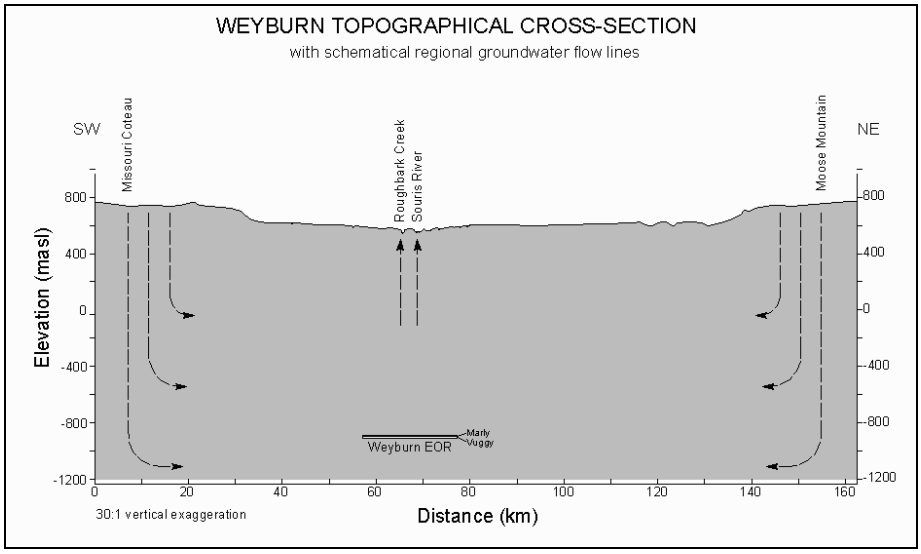

Fig. 5 Topographical cross-section A-B from Missouri Coteau to Moose Mountain with elevation differences well in excess of 200 m. The elevations have been taken from the 1:250,000 and, in the Weyburn area, from the 1:50,000 NTDB maps. For location of cross-section, see Fig. 3.

The regional recharge areas for the deep-penetrating regional flow systems are in the topographical highlands (the Missouri Coteau about 40 km to the southwest of the Weyburn Project and Moose Mountain and elevated neighbouring areas to the northeast). The elevation differences of more than 200 m between the bordering highlands and the regional discharge area in the immediate valley of the Souris River (Fig. 3) are sufficient to propel groundwater flow systems to the depths of the Weyburn field. The field is located in the regional discharge area with upward-directed flow (before production of the field). The lateral extent of the cross-section is approximately 160 km.

The topographical situation at the Zama site (Figs. 6, 7 and 8) is principally similar to the Weyburn site. The regional recharge areas are the Clear Hills Uplands to the south of the Fort Nelson Lowlands and the Camaron Hills Uplands to the North. The Zama EOR project is mainly located within the Fort Nelson Lowland. The elevation differences between the recharge areas in the upland and the discharge areas (before petroleum production) in the lowlands (Zama Lake) reach 450 m. The lateral extent of the cross-section is approximately 180 km.

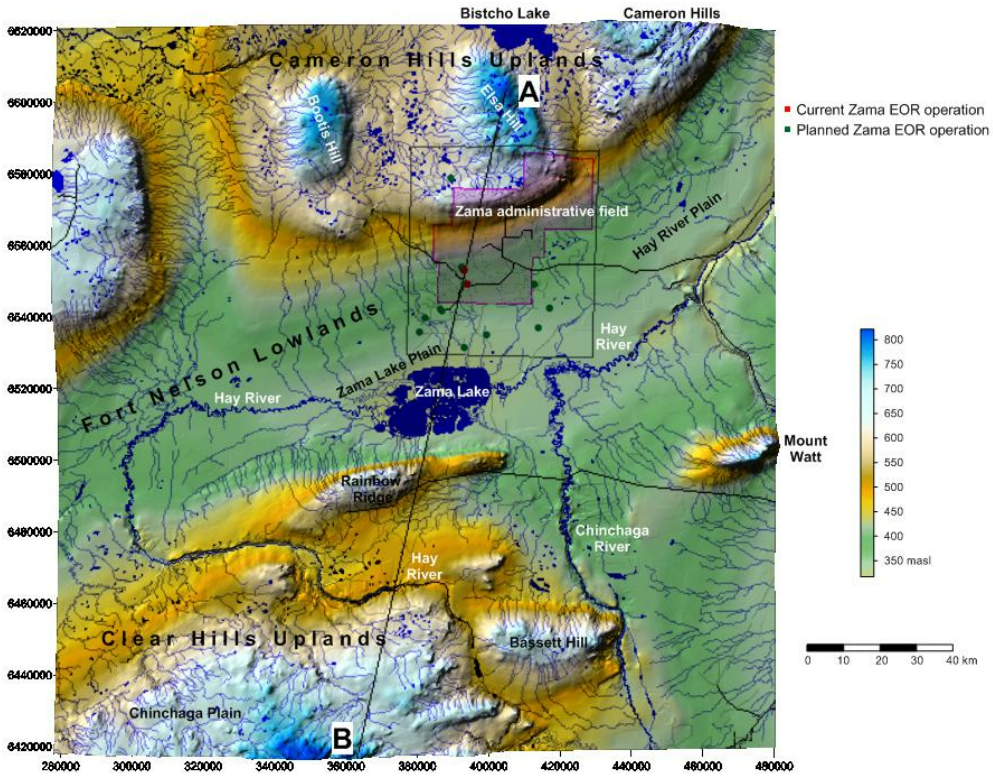

Fig. 6 Bird's-eye view of the DEM for the general Zama Lake area based on NTDB 1:250,000 digital maps 084E (Chinchaga River),084F (Bison River), 084K (Mount Watt), 084L (Zama Lake), 084M (Bistcho Lake), 084N (Steen River), 094H (Beatton River), 094I (Fontas River) and 094P (Petitat River). The topographical cross-section A-B is shown in Fig. 8.

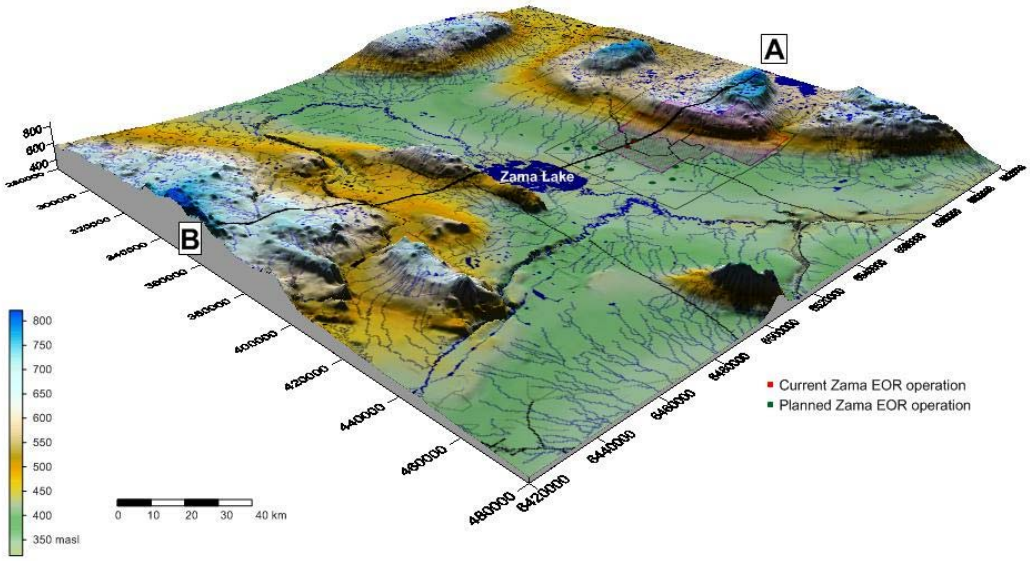

Fig. 7 Oblique view of the DEM for the general Zama project area. The Zama EOR is topographically located in a regional lowland (regional discharge area) flanked to the north by the Cameron Hills Uplands and to the south by the Clear Hills Uplands (regional recharge areas).

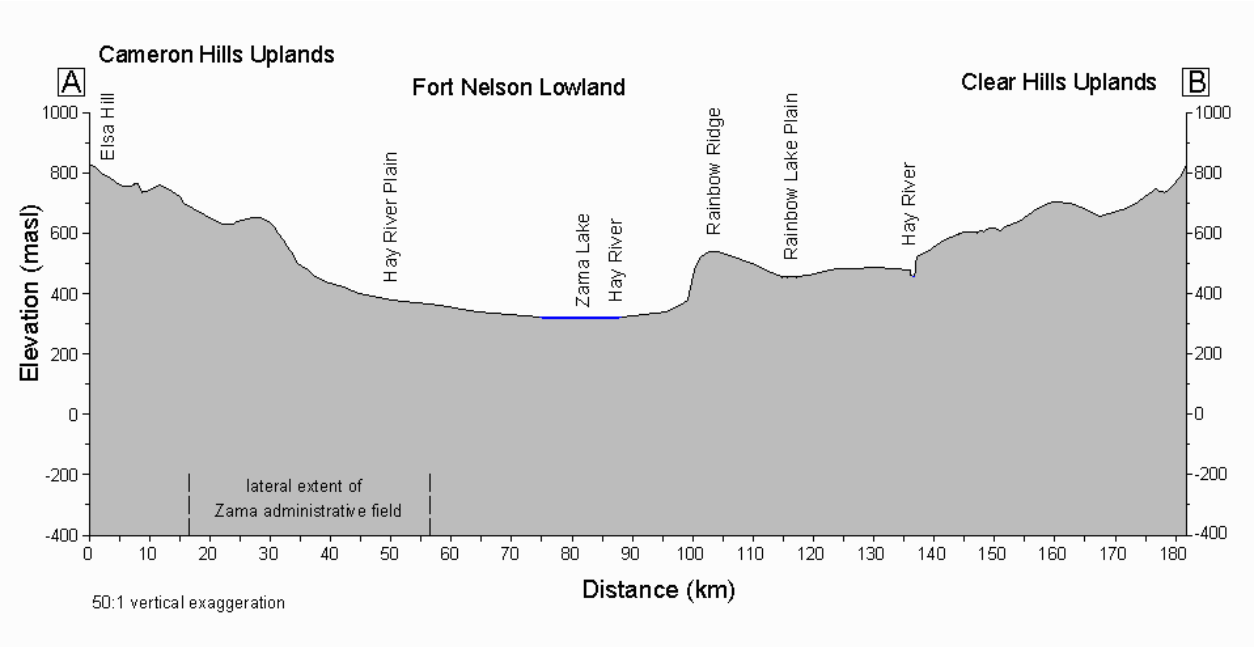

Fig. 8 Topographical cross-section A-B from the Clear Hills Uplands to the Cameron Hills Uplands with elevation differences in excess of 400 m. The elevations have been taken from 1:250,000 maps. For location of cross-section, see Fig. 6 and 7.

The topographical situation at the Wabamun site (Figs. 9, 10 and 11) is more complex than the previously described Weyburn and Zama sites. The total Study Area is outlined in red, the Focus Area in black. The regional recharge areas are between the North Saskatchewan River, Gull Lake, and Pigeon Lake. The valley of the North Saskatchawan River and possibly the low area of Pigeon Lake are the recipients of deep-seated regional groundwater flow. In the total Study Area, the elevation differences between the recharge areas in the upland and the discharge area North Saskatchewan River reach approximately 400 m over a distance of about 70 km. The complete lateral extent of the cross-section A-B is approximately 100 km. In the Focus Area the highest elevation id approximately 920 masl and the nearest discharge point in the valley of the North Saskatchewan River has an elevation of approximately 660 masl at a distance of about 30 km. The maximum elevation difference of the groundwater table in the Focus Area to the North Saskatchewan River is approximately 250 m over a distance of about 30 km and could well establish deep groundwater flow systems under natural conditions.

It is self-apparent that the hydrostatic flow behaviour of CO_2 at the Sleipner site cannot be applied at the Weyburn, Wabamun and Zama sites or other on-shore sites dominated by hydrodynamic flow behaviour of hydrous fluids and CO_2.

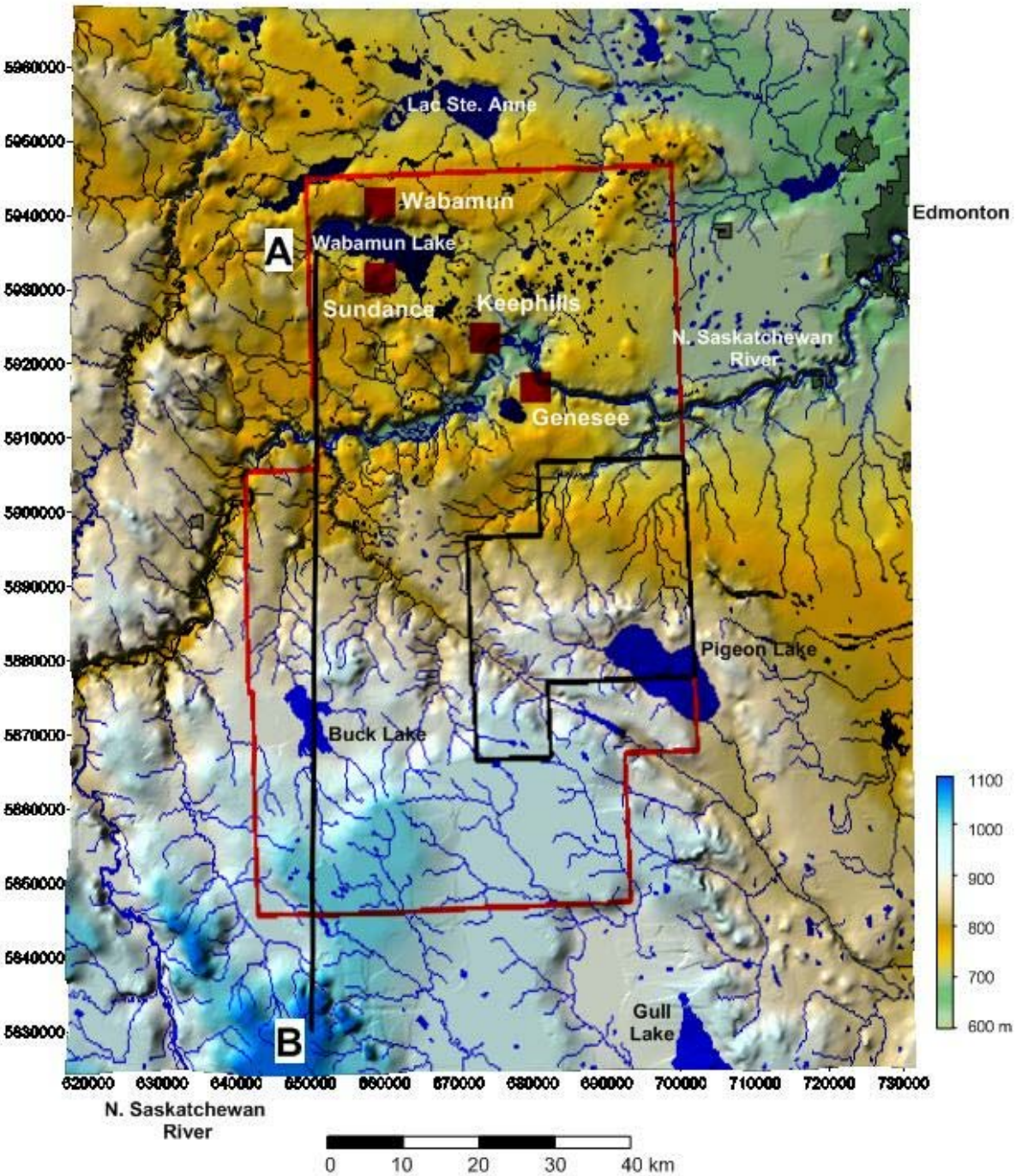

Fig. 9 Bird's-eye view of the DEM for the Wabamun Area CO_2 Sequestration Project (WASP) study area based on NTDB 1:250,000 digital maps 083A (Red Deer), 083B (Rocky Mountain House), 083G (Wabamun Lake) and 083H (Edmonton). The topographical cross-section A-B is shown in Fig. 11. The red squares indicate the location of coal power plants supplying the CO_2 for injection. The red outline denotes the total Study Area, the black one the Focus Area.

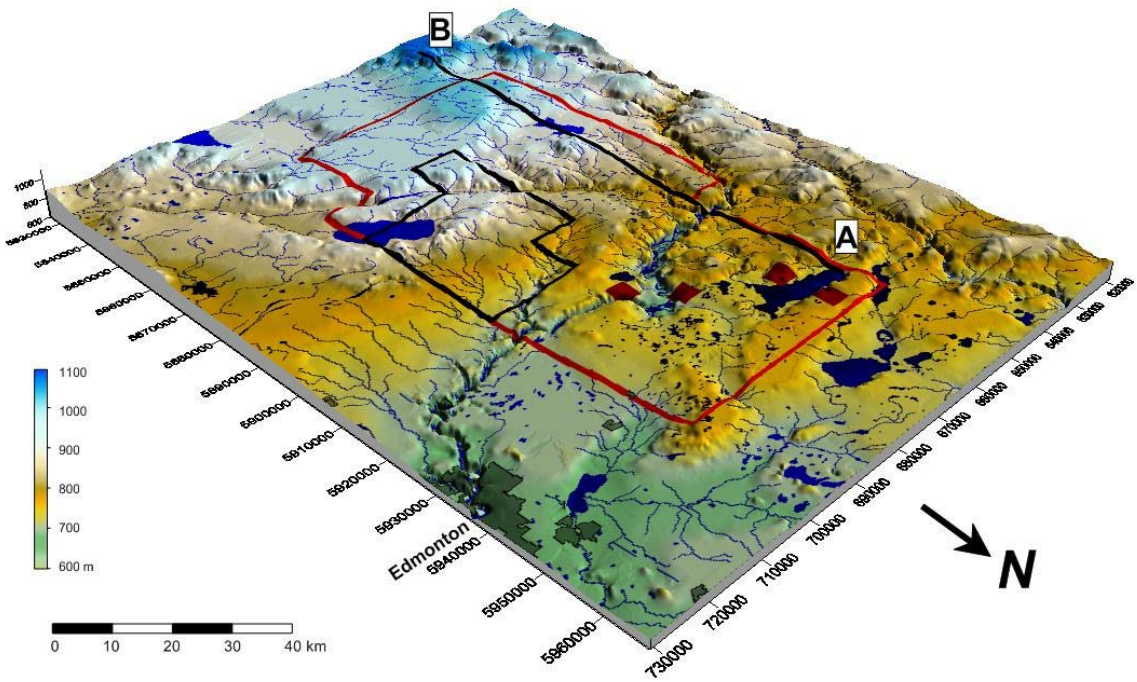

Fig. 10 Oblique view of the DEM for the general WASP area.The WASP study area is located in a complex topographical setting with regional discharge areas along the North Saskatchewan River and possibly also Pigeon Lake.

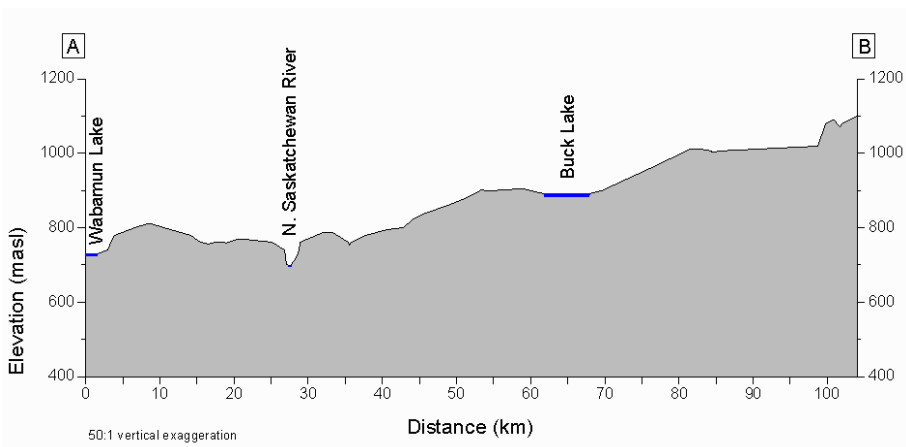

Fig. 11 Topographical cross-section A-B from the upland near endpoint B to Wabamun Lake with elevation differences of approximately 400 m. The elevations have been taken from 1:250,000 maps. For location of cross-section, see Fig. 9.

Another point requiring attention is that some of the present fluid flow programs in hydrogeology and many of the simulators in petroleum work assume the buoyancy of hydrostatic conditions. They may work reasonably well for hydrostatic situations as encountered at the Sleipner CO_2 injection site though this needs, however, to be verified as far as the application of physical causality is concerned, in particular with respect to the assumption of grad p as the driving force for fluid flow. These simulators would not be well-suited to investigate any large scale on-shore CO_2-injection (as for instance at the Weyburn, Zama, and Wabamun CO_2 injection sites). In general, present simulators and some groundwater programs

need to take into account the proper physics of fluid flow, in particular the inclined direction of the pressure potential force and any occurrence of *Buoyancy Reversal*.

It appears that on-shore regional recharge areas may be good targets for CO_2 injection as naturally-occurring BR may provide an additional hydraulic trapping mechanism for the geologic storage of CO_2 as outlined in chapter 5. The size of recharge areas is usually much larger than that of the associated discharge areas.

The goal should be to undertake holistic investigations of the complete underground fluid flow systems from the groundwater table to the depths achieved by natural flow systems and of those systems modified by hydrocarbon production and, at a later stage, large scale carbon injection.

References

Chalaturnyk, R.J. and K.E.Durocher, 2006. The Weyburn CO2 monitoring and storage project. Case study of a CO2-EOR storage project. APEC CO2 Capture and Storage Capacity Building Workshop, Beijing, Oct. 2006.

Keith, D. and R. Lavoie, 2009. An overview of the Wabamun area CO_2 Sequestration Project (WASP). Energy Procedia 1 (2009), pp. 2817-2824.

Smith, S.A., J.A. Sorenson, E.N. Steadman, J.A. Harju, W.A. Jackson, D. Nimchuk, and R. Lavoie, 2007. Zama acid gas EOR, CO2 sequestration and monitoring project. Proceeedings of the 6th Annual Conference on Carbon Capture & Sequestration, Pittsburg, 2007. 13 p.

Weyer, K.U., 1978. Hydraulic forces in permeable media. Mémoires du B.R.G.M., vol. 91, p.285 - 297, Orléans, France *[available from http://www.wda-consultants.com]*

Weyer, K.U., 1996. Darlegung und Anwendung der Dynamik von Grundwasserfließsystemen auf die Migration von gelösten Schadstoffen im Grundwasser [Physics of groundwater flow and its application to the migration of dissolved contaminants]. Final Research report to the Federal Environmental Office of the German Government. 204 pages, 79 fig., 16 photographs, 15 tab. [in German]: April 1996 [*available from http://www.wkc-consultants.com*].

Weyer, K.U., 2006a. Industrial waste disposal site Münchehagen: Confinement of dissolved contaminants by discharging saline water. Revised version of paper originally submitted to Solutions '95, Congress of International Association of Hydrogeologists, Edmonton, Alberta, Canada, June 4-10, 1995, 9 pages [*available from http://www.wda-consultants.com*].

Weyer, K.U., 2006b. Monitoring piezometers in recharge areas: Is one 'upstream' and two 'downstream' adequate. Revised version of paper originally submitted to Solutions '95, Congress of International Association of Hydrogeologists, Edmonton, Alberta, Canada, June 4-10, 1995, 9 pages [*available from http://www.wda-consultants.com*].

Chapter 8

Roadmap

K. Udo Weyer
WDA Consultants Inc., Calgary, AB, Canada
weyer@wda-consultants.com

The application of Hubbert's Force Potential and the Theory of Groundwater Flow Systems will open new dimensions and bring more clarity to geological storage and the prediction of long term migration of CO_2 . Chapters 1 to 7 above established a need for modelling of CO_2 sequestration by model codes based on these theories. The following outline lists a number of investigations to advance the manner in which these methods can be applied to the geological storage of CO_2. (The sequence of the list does not imply a chronological order.)

1. Evaluation of pre-production, production and post-production pressure and head recordings of selected oil and gas fields with and without EOR operation. Historical and present oil field pressure data should also be evaluated for the presence and extent of natural BR occurrences as well as those which have been created by hydrocarbon production. This task should be commenced without delay. The occurrence of BR is widespread within oil fields and the available data need to be re-examined and re-interpreted accordingly.

2. Regional saline aquifers systems should be investigated to locate layers possibly exhibiting BR and to determine the areas with natural upwards and downward directed cross-formational flow directions within overlying aquitards and caprocks. In a first step, the equipotential lines and flow directions of deep groundwater flow systems can be determined using 2D vertical mathematical models if general geological cross-sections can be constructed or are already available. Weyer, 1996, in a research project for the Environmental Office (Umweltbundesamt) of the German Federal Government, successfully applied such modelling of groundwater flow to determine the depth and approximate gradients of the gravitational groundwater flow systems within regional aquifers and aquitards. This was accomplished without dedicated deep borehole data but based solely on geologic cross-sections from public 1:25,000 geological maps and the estimate of contrast permeabilities for all geological layers. The research report should be translated into English in order to make the methodology available to a larger audience.

   In a second step, the results of the 2D-vertical mathematical modelling should then be verified with a very limited number of strategically-emplaced deep boreholes.

3. Evaluation and extension of codes.
   A. Existing simulation codes should be evaluated and tested to ensure a physically-correct application of Hubbert's Force Potential and the Theory of Groundwater Flow Systems.
   B. A pre- and post-processor system should be written for the latest version of FLONET, an available and well-tested 2D program for groundwater flow in geological cross-sections. This would make the program and the implied methodology accessible to a wider audience concerned with CO_2 sequestration.

4. Model studies (using hydrogeological codes)
   A. Frind and Molson (2010) concur that a series of 2D cross-sectional flownet models should be conducted to narrow the conditions under which "buoyancy reversals" do occur. These studies should be based on the actual topography and geology at present and future CO_2 pilot sites. The use of contrast permeabilities is proposed and sufficient to determine the flow directions (Weyer, 1996) and the occurrence of *Buoyancy Reversal*.
   B. Successful 2D-flow model simulations in geologic cross-sections should be augmented by 3D models again by assuming contrast permeabilities.
   C. Flow modelling of trapping CO_2 by means of *Buoyancy Reversal* should be tested and developed further by applying an advanced multiphase flow model. Appropriate simulations would provide insights into various critical issues such as the duration of pumping required, the long-term effectiveness of the method in sequestering the CO_2 , and the economics of the scheme.

5. Construction of a physical table model (consisting of three layers in a sand model, or their equivalent in a Hele Shaw arrangement or a vertically arranged Venturi flume) to demonstrate the occurrence and effect of *Buoyancy Reversal.* Injection of sufficiently light parcels would cause upward movement within the aquifers above and below the aquitard and downwards within the aquitard.

6. Preparation of a manual on the application of Hubbert's mechanical force fields to carbon sequestration.

Appendix 1

Review of "Physical Processes in Carbon Storage" by Udo Weyer

Reviewed by E.O. Frind[(1)] and J.W. Molson[(2)], 16 pages
January 11, 2010

Summary

We have briefly reviewed this paper consisting of 7 chapters plus a slide show, focusing on the text portion. The main thrust of the paper is that there exists a physical process the author chooses to give the term *Buoyancy Reversal*, and that this process can be used to advantage in the sequestration of CO_2 in geologic formations. In addition, the author has identified a number of deficiencies in conventional subsurface modelling techniques.

Our review shows that *Buoyancy Reversal* exists, although we might choose a slightly different term to describe this phenomenon. This phenomenon is a natural physical process, and the conditions under which it occurs can be readily predicted. Any groundwater model based on sound fundamental theories should be able to predict *Buoyancy Reversal* under the appropriate conditions.

With regard to modelling deficiencies, we are confident that standard techniques used in hydrogeology, at least as far as models originated and developed at the University of Waterloo are concerned, are sound. The development of groundwater models at Waterloo started under the direction of the first reviewer in the 1970s, initially in close cooperation with George Pinder at Princeton University. Our models are based on, and are consistent with, the fundamental theories postulated by Hubbert (1940).

We cannot comment on the validity of reservoir simulation models used in the oil industry. However, on the basis of the evidence presented by the author, we agree that certain reservoir simulation models may have deficiencies which would make them unsuitable for application to groundwater systems, including CO_2 sequestration.

Affiliation of reviewers:
[(1)] University of Waterloo, Waterloo, Ontario, Canada
[(2)] Laval University, Quebec City, Quebec, Canada

The full review including 16 pages of detailed comments and results of 1D and 2D modelling of *Buoyancy Reversal* by means of hydrogeological computer programs is available from

http://www.wda-consultants.com/co2-main.htm
